

AD-A240 766



UTIC



## Leveling of the AMBLER Walking Machine: A Comparison of Methods

Pablo Gonzalez de Santos

Peter V. Nagy

William L. Whittaker

CMU-RI-TR-91-13

THE ROBOTICS INSTITUTE  
CARNEGIE MELLON UNIVERSITY  
Pittsburgh, PA 15213-3890

July 1991

91-11002

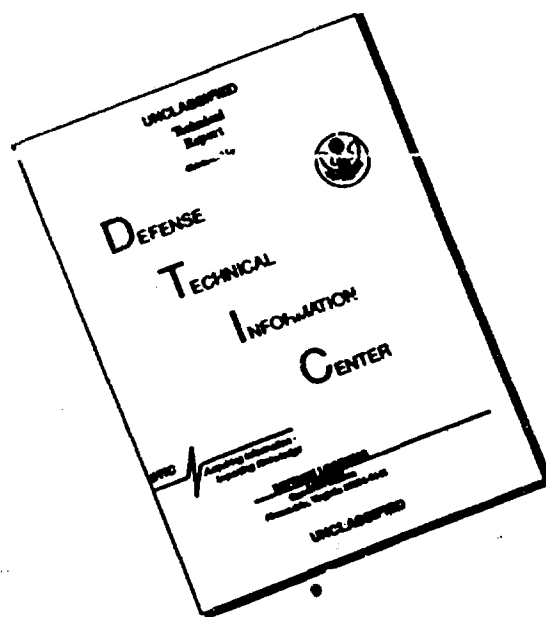


© 1991 Carnegie Mellon University

This research was sponsored by NASA under Grant NAGW-1175. The views and conclusions contained in this document are those of the authors and should not be interpreted as representing the official policies, either expressed or implied, of NASA or the United States Government.

01 0 18 060

# DISCLAIMER NOTICE



**THIS DOCUMENT IS BEST  
QUALITY AVAILABLE. THE COPY  
FURNISHED TO DTIC CONTAINED  
A SIGNIFICANT NUMBER OF  
PAGES WHICH DO NOT  
REPRODUCE LEGIBLY.**

# REPORT DOCUMENTATION PAGE

Form Approved  
OMB No. 0704-0188

Public reporting burden for this collection of information is estimated to average 1 hour per response, including the time for reviewing instructions, searching existing data sources, gathering and maintaining the data needed, and completing and reviewing the collection of information. Send comments regarding this burden estimate or any other aspect of this collection of information, including suggestions for reducing this burden, to Washington Headquarters Services, Directorate for Information Operations and Reports, 1215 Jefferson Davis Highway, Suite 1204, Arlington, VA 22202-4302, and to the Office of Management and Budget, Paperwork Reduction Project (0704-0188), Washington, DC 20503.

1. AGENCY USE ONLY (Leave blank)	2. REPORT DATE July 1991	3. REPORT TYPE AND DATES COVERED technical	
4. TITLE AND SUBTITLE Leveling of the AMBLER Walking Machine: A Comparison of Methods		5. FUNDING NUMBERS Grant NAGW-1175	
6. AUTHOR(S) Pablo Gonzalez de Santos, Peter V. Nagy, and William L. Whittaker			
7. PERFORMING ORGANIZATION NAME(S) AND ADDRESS(ES) The Robotics Institute Carnegie Mellon University Pittsburgh, PA 15213		8. PERFORMING ORGANIZATION REPORT NUMBER  CMU-RI-TR-91-13	
9. SPONSORING MONITORING AGENCY NAME(S) AND ADDRESS(ES)  NASA		10. SPONSORING MONITORING AGENCY REPORT NUMBER	
11. SUPPLEMENTARY NOTES			
12a. DISTRIBUTION AVAILABILITY STATEMENT  Approved for public release; Distribution unlimited		12b. DISTRIBUTION CODE	
13. ABSTRACT (Maximum 200 words) For orthogonally-decoupled machines, such as the AMBLER, power efficiency is contingent upon keeping the body level. There are several ways of accomplishing this, which trade-off approximations of the complete phenomena versus simplicity of the implementation. In this report the effectiveness of four different strategies are evaluated for body attitude control. One of these uses vertical actuations to level the body ignoring the secondary geometric effects. Two alternate methods actuate only the vertical axes, but additionally utilize part of the horizontal kinematic information to calculate the required vertical displacements. Another method actuates both the horizontal and vertical joints in order to obtain ideally correct kinematic motion, but at the cost of higher energy expenditure. In this document the simulation of these methods and their implementation on the AMBLER are reported.  This research shows that leveling methods that use only the vertical axes are most appropriate. The Simple Z-axes leveling method works satisfactorily to level using only six concurrent motions, ignoring the complexity of higher order kinematic calculations. The Z-axes method that is derived from the All-axes method has the consequence that the body drops when these equations are used to tilt the body. The Isoaltitude method performs slightly better than the Simple Z-axes method, by maintaining constant body height during both leveling and tilting maneuvers.			
14. SUBJECT TERMS		15. NUMBER OF PAGES 38 pp	16. PRICE CODE
17. SECURITY CLASSIFICATION OF REPORT unlimited	18. SECURITY CLASSIFICATION OF THIS PAGE unlimited	19. SECURITY CLASSIFICATION OF ABSTRACT unlimited	20. LIMITATION OF ABSTRACT unlimited

# Contents

<b>1. Introduction</b> .....	1
<b>2. The Leveling Equations</b> .....	4
<b>2.1 All-axes-leveling Method</b> .....	4
2.1.1 Deriving the Leveling Equations by Using Projection.....	4
2.1.2 Deriving the Leveling Equations by Using Rotation Matrices .....	8
<b>2.2 Z-axes-leveling Methods</b> .....	10
2.2.1 Simple Z-axes-leveling Method.....	10
2.2.2 Z-axes-leveling Method from the All-axes-leveling Method.....	11
2.2.3 Isoaltitude Z-axes-leveling Method .....	11
<b>3. Kinematic Simulations</b> .....	14
<b>3.1 All-axes-leveling Method</b> .....	14
<b>3.2 Z-axes-leveling Method</b> .....	22
3.2.1 Simple Z-axes-leveling Method .....	22
3.2.2 Z-axes-leveling Method from the All-axes-leveling Method.....	24
3.2.3 Isoaltitude Z-axes-leveling Method.....	26
3.2.4 Foot Slippage .....	27
<b>4. Implementation of Leveling Control on the AMBLER</b> .....	31
<b>4.1 All-axes-leveling Method</b> .....	31
<b>4.2 Z-axes-leveling Methods</b> .....	32
<b>4.3 Power Consumption Measurements</b> .....	33
<b>5. Conclusion</b> .....	37
<b>6. References</b> .....	38

# List of Figures

1. The AMBLER walking machine .....	1
2. An Ambler leg .....	2
3. A circular gait .....	3
4. Projection of two legs onto the plane YZ .....	4
5. Projection of two legs onto the plane $\bar{x}\bar{z}$ .....	6
6. An Ambler leg in two configurations.....	8
7. Diagram of the Ambler-equivalent leg .....	9
8. Rotations required to level the body .....	11
9. Motion of a leg for the Isoaltitude Z-axes-levelingmethod .....	12
10. Superposition of the Ambler-equivalent model at $\theta = 5^\circ$ and $\theta = 0^\circ$ for $\gamma = 0^\circ$ .....	15
11. Ambler-equivalent model at $\theta = 5^\circ$ and $\gamma = 0^\circ$ .....	16
12. Ambler-equivalent model at $\theta = 0^\circ$ and $\gamma = -5^\circ$ .....	17
13. Ambler-equivalent model at $\theta = 5^\circ$ and $\gamma = -5^\circ$ .....	18
14. The X coordinates and their incremental changes during leveling .....	19
15. The Y coordinates and their incremental changes during leveling .....	20
16. The Z coordinates and their incremental changes during leveling.....	21
17. Displacement of the body frame, knee, and hip when using the the Simple Z-axes method .....	22
18. Displacement of the body frame for for different initial tilts when using the Simple Z-axes-leveling method .....	23
19. Displacement of the body frame, knee, and hip when using the Z-axes-leveling method from the All-axes-leveling method.....	24
20. Displacement of the body frame for different initial tilts when using the Z-axes-leveling method from the All-axes-leveling method.....	25
21. A sequence of tilting and leveling using the Z-axes-leveling method from the All-axes-leveling method.....	26
22. Displacement of the body frame, knee, and hip when using the Isoaltitude Z-axes-leveling method.....	27
23. Plan view of the AMBLER at level (solid line) and at a tilt (dotted line) of $\theta = -5^\circ$ and $\gamma = 5^\circ$ .....	28
24. Maximum difference between leg extensions .....	30
25. Attitude change during leveling for the All-axes-leveling method .....	31
26. Attitude change during leveling for the Simple Z-axes-leveling method .....	32
27. Attitude change during leveling for Z-axes-leveling method from the All-axes-leveling method.....	33
28. Raw data (dashed line) and filtered data (solid line) for a leveling using the All-axes-leveling Method .....	34
29. Power consumption for leveling the AMBLER from $\theta = 3^\circ$ and $\gamma = 3^\circ$ .....	35
30. Power consumption for leveling the AMBLER from $\theta = 5^\circ$ and $\gamma = 5^\circ$ .....	35

## List of Tables

1. Initial foot positions and link lengths at level for the Ambler-equivalent model.....	15
2. Link lengths at an initial tilt of $\theta = 5^\circ$ and $\gamma = 0^\circ$ and link increments to level the body .....	16
3. Link lengths at an initial tilt of $\theta = 5^\circ$ and $\gamma = -5^\circ$ and link increments to level the body .....	17
4. Link lengths at an initial tilt of $\theta = -5^\circ$ and $\gamma = -5^\circ$ and link increments to level the body.....	18
5. Data to level the body from an initial tilt of $\theta = 5^\circ$ and $\gamma = -5^\circ$ .....	29
6. Foot slippage for leg 5 under variations of the extension on leg 0 .....	30
7. Power meter data during the experiments .....	36

## Abstract

For orthogonally-decoupled machines, such as the AMBLER, power efficiency is contingent upon keeping the body level. There are several ways of accomplishing this, which trade-off approximations of the complete phenomena versus simplicity of the implementation. In this report the effectiveness of four different strategies are evaluated for body attitude control. One of these uses vertical actuations to level the body ignoring the secondary geometric effects. Two alternate methods actuate only the vertical axes, but additionally utilize part of the horizontal kinematic information to calculate the required vertical displacements. Another method actuates both the horizontal and vertical joints in order to obtain ideally correct kinematic motion, but at the cost of higher energy expenditure. In this document the simulation of these methods and their implementation on the AMBLER are reported.

This research shows that leveling methods that use only the vertical axes are most appropriate. The Simple Z-axes leveling method works satisfactorily to level using only six concurrent motions, ignoring the complexity of higher order kinematic calculations. The Z-axes method that is derived from the All-axes method has the consequence that the body drops when these equations are used to tilt the body. The Isoaltitude method performs slightly better than the Simple Z-axes method, by maintaining constant body height during both leveling and tilting maneuvers.

# 1. Introduction

Since 1987, The CMU Planetary Rover Group has been developing an autonomous vehicle for planetary exploration sponsored by NASA [1], [2]. The main goal of this group is to develop technologies for autonomous robots on unstructured, natural terrain.

A legged mechanism was chosen to achieve this for a number of reasons:

- Legged vehicles can negotiate rugged terrain, such as crossing ditches and going over obstacles.
- Legs provide discrete footfall placement; consequently, their ground contacts are predictable and energy-efficient.
- Legs can aid positioning and orienting sensors and scientific observation sampling equipment.

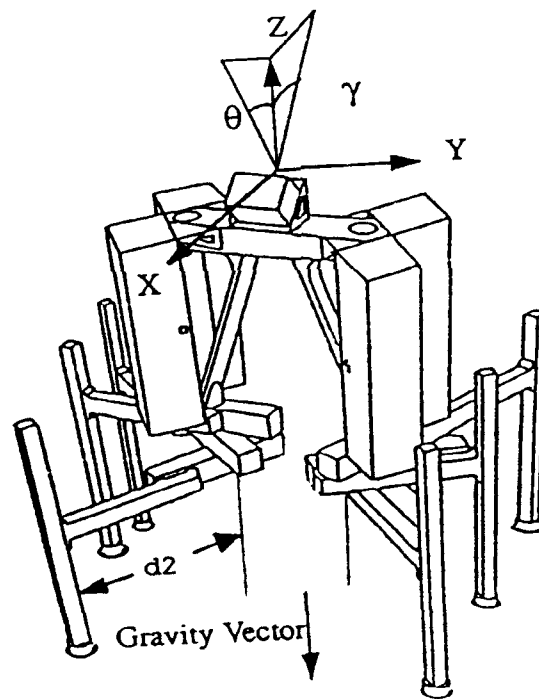


FIGURE 1. The AMBLER walking machine

Our group has designed and built a six-legged walking machine named AMBLER<sup>1</sup> depicted in Figure 1. This machine has three orthogonal legs stacked under the main body on each of the two central shafts. Each leg consists of a rotational joint, two horizontal links (inner and outer) with a prismatic joint connecting them, and a vertical link attached to the outer link with another prismatic joint (see Figure 2).

<sup>1</sup> Autonomous MoBiLe Exploration Robot

This resulting configuration leads to a novel *circulating gait* unprecedented in existing walking mechanisms or the animal kingdom. This gait consists of raising a leg, moving it through both stacks, and placing it in front of the fore leg of its stack; this procedure is called *leg recovery*. After every six leg recoveries, all legs have completed a full revolution about its respective body shaft (see Figure 3).

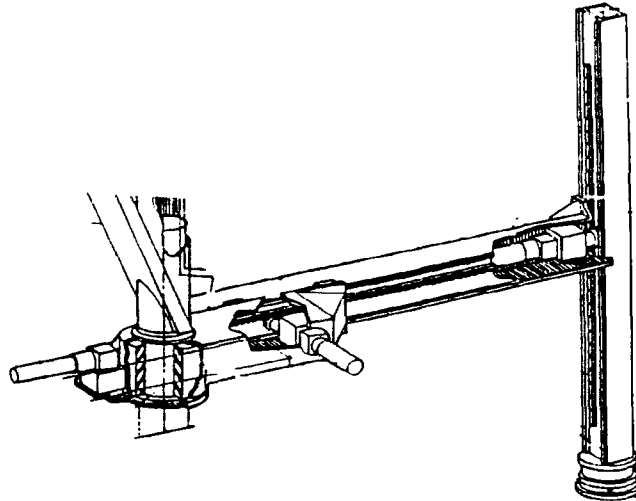


FIGURE 2. An Ambler leg

The Ambler leg possesses several advantages:

- Decoupling horizontal from vertical motions. Therefore it is more energy efficient by precluding the so-called *negative work* effect, and also eliminates gravity loading from many joints.
- The orthogonal leg is ideally suited for rough terrain as the vertical links sweep no significant volume during propulsion and consequently may be placed close to obstacles.
- A circular gait needs only one third of the foot placements than traditional terrain-adaptive gaits. For example, the AMBLER needs to take only six steps to advance the body as far as a similar-sized walker would need eighteen.

The AMBLER integrates perception, planning, and control, using the Task Control Architecture (TCA) [11], which provides interprocessor communication, task synchronization, and resource management. The perception system placed on the top of the body is a scanning laser rangefinder, which measures both reflectance and range. It supplies 3D data more rapidly and reliably than passive vision techniques such as binocular stereo with motion [7], [8], [12].

The eighteen actuators of the AMBLER are permanent magnet DC motors and they are controlled by nine motion control boards which provide the user with programmable PID and feedforward gains and a trajectory tracking command to follow joint trajectories. The boards are commanded by a MC68020 processor which communicates with a MC68030 master processor

through shared memory using semaphores. Both processors run under VxWorks, a real-time multitasking environment.

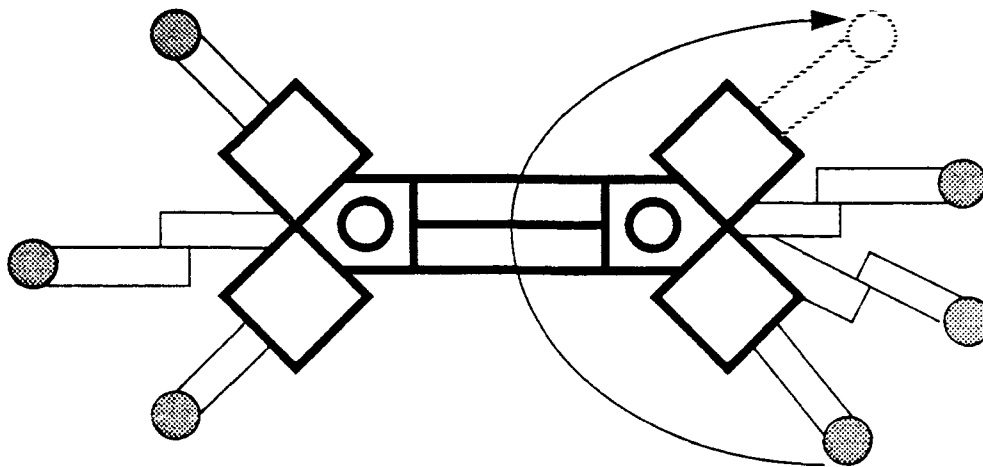


**FIGURE 3.** A circular gait

The AMBLER has inclinometers which are used to monitor body attitude, and a force sensor on each foot which provides the forces and moments on three orthogonal axes. These sensors give the machine the capability of detecting several conditions on the leg-ground surface [9]. These sensors, combined with the feet and body c.g. location, will constitute the main elements of the AMBLER safeguard monitor.

The AMBLER was designed to walk with a level body. This decreases the power needed to propel the body and simplifies perception, planning and control. However, the tilt of the AMBLER changes during its movement for reasons such as different compaction of the soil it steps on and leg support failures. Therefore, it is necessary to check and correct the tilt of the body on a regular basis.

In this report four sets of kinematic equations for leveling the AMBLER are developed and compared. Three of them use only the vertical actuators with small angle approximations [6]; the other, which is more accurate, requires the movement of all actuators at the same time. The phenomena that are compared are: body translation, foot slippage, and power consumption. All of the methods that use only the vertical actuators incur significant horizontal body translation and are more likely to give rise to foot slippage. Some of these methods also cause a smaller displacement of the body in the vertical direction. The method that uses all axes to level the body avoids foot slippage and body translation at the cost of higher energy expenditure. The small difference in energy expenditure among the three Z-axes only leveling methods is attributed to the difference in vertical body excursions among them.

## 2. The Leveling Equations

To level the AMBLER, joint motions are planned and executed to bring the plane XY of the body reference system to horizontal. Therefore, the final rotations about the X and Y axes are zero. These angles can be obtained from inclinometers which give the angles that the X and Y axes of the body have with the gravity vector. These angles are independent of one another because the sensors are built to ignore rotation outside of the sensor plane.

### 2.1 All-axes-leveling Method

One technique to derive the All-axes-leveling equations uses projections of the legs onto the planes XZ and YZ. The other technique uses rotation transformations to achieve the same result. The first one is more graphic, and it is similar to the derivation of the Isoaltitude Z-axes leveling method.

#### 2.1.1 Deriving the Leveling Equations by Using Projections

To derive the leveling equations, leg  $i$  is projected onto the plane YZ. Let  $y_i$  and  $z_i$  be the coordinates of the leg  $i$  in the body reference system. The length of the vertical link will be  $|z_i|$ , and the length of the horizontal link will be  $\sqrt{y_i^2 + (y_i - d)^2}$  in terms of an Ambler leg (see Figure 2). If the tilt,  $\theta$ , of the body about the X axis changes, then the coordinates of each leg should change in such a way that the body reference frame,  $O$ , and the feet do not move (see Figure 4). As a consequence, segments  $a_i$  and  $b_i$  do not change. Similarly, for leg  $j$ , segments  $a_j$  and  $b_j$  do not change.

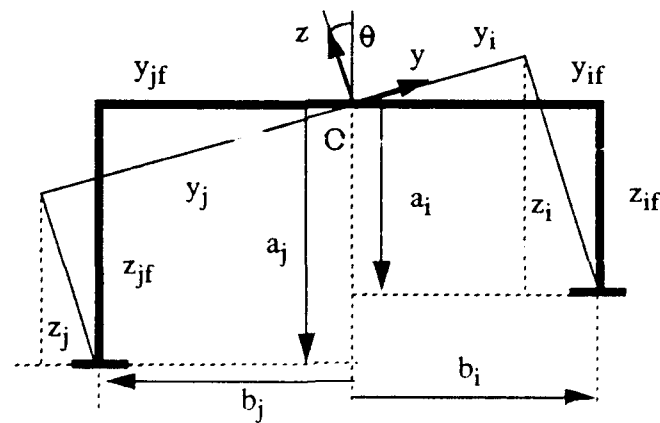


FIGURE 4. Projection of two legs onto the plane YZ

Referring to Figure 4, the length of these segments for leg  $i$  are:

$$a_i = y_i \sin \theta + z_i \cos \theta \quad (1)$$

$$b_i = y_i \cos \theta - z_i \sin \theta \quad (2)$$

The same equations apply to leg  $j$  on the other stack by switching subscripts. These equations can be re-written in matrix form as:

$$A(\theta) \bar{w}_i = \bar{e}_i \quad (3)$$

where

$$A(\theta) = \begin{bmatrix} \sin\theta & \cos\theta \\ \cos\theta & -\sin\theta \end{bmatrix} \quad (4)$$

$$\bar{w}_i = \begin{bmatrix} y_i \\ z_i \end{bmatrix} \quad (5)$$

$$\bar{e}_i = \begin{bmatrix} a_i \\ b_i \end{bmatrix} \quad (6)$$

When the body tilts about the x-axis from  $\theta_1$  to  $\theta_2$ , then for leg  $i$ :

$$A(\theta_2) \bar{w}_{i,2} = A(\theta_1) \bar{w}_{i,1} \quad (7)$$

and the new leg coordinates will be:

$$\bar{w}_{i,2} = A^{-1}(\theta_2) A(\theta_1) \bar{w}_{i,1} \quad (8)$$

Since  $A(\theta)$  is an *orthogonal* matrix, its inverse always exists and is the same as itself, i.e.  $A^{-1}(\theta) = A(\theta)$ . Thus, the initial and final leg coordinates are related to the change in tilt as follows:

$$\bar{w}_{i,2} = \begin{bmatrix} \sin\theta_2 & \cos\theta_2 \\ \cos\theta_2 & -\sin\theta_2 \end{bmatrix} \begin{bmatrix} \sin\theta_1 & \cos\theta_1 \\ \cos\theta_1 & -\sin\theta_1 \end{bmatrix} \bar{w}_{i,1} \quad (9)$$

which gives:

$$\bar{w}_{i,2} = \begin{bmatrix} \cos\theta & \sin\theta \\ -\sin\theta & \cos\theta \end{bmatrix} \bar{w}_{i,1} \quad (10)$$

where  $\theta = \theta_2 - \theta_1$ .

Additionally, the increment between the final and initial position of a leg  $\Delta w_i = w_{i,2} - w_{i,1} = \begin{bmatrix} \Delta y_i \\ \Delta z_i \end{bmatrix}$  can be written as:

$$\Delta w_i = \begin{bmatrix} \cos\theta - 1 & \sin\theta \\ -\sin\theta & \cos\theta - 1 \end{bmatrix} w_{i,1} \quad (11)$$

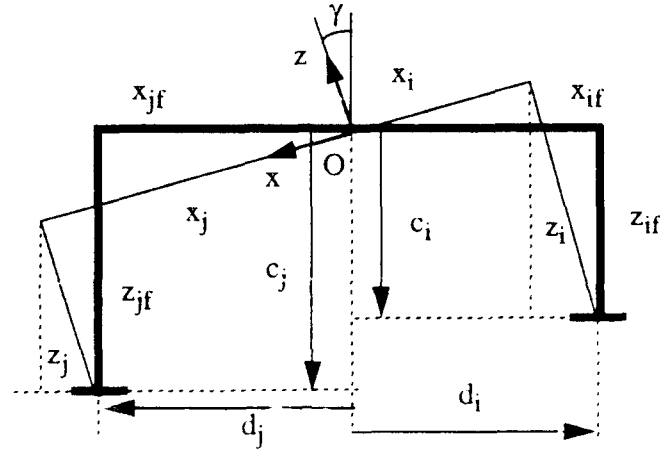


FIGURE 5. Projection of two legs onto the plane XZ

With the projection of the leg onto the plane XZ the same steps are followed, being careful to follow the right hand rule in defining the positive angle of rotation as shown in Figure 5. For leg  $i$  the constant-length segments are:

$$c_i = -x_i \sin \gamma + z_i \cos \gamma \quad (12)$$

$$d_i = x_i \cos \gamma + z_i \sin \gamma. \quad (13)$$

The same equations apply to leg  $j$  on the other stack by switching subscripts. These equations may be re-written in matrix form as:

$$B(\gamma) \bar{u}_i = \bar{f}_i \quad (14)$$

where

$$B(\gamma) = \begin{bmatrix} -\sin \gamma & \cos \gamma \\ \cos \gamma & \sin \gamma \end{bmatrix} \quad (15)$$

$$\bar{u}_i = \begin{bmatrix} x_i \\ z_i \end{bmatrix} \quad (16)$$

$$\bar{f}_i = \begin{bmatrix} c_i \\ d_i \end{bmatrix}, \quad (17)$$

and the new leg coordinates when the body tilts from  $\gamma_1$  to  $\gamma_2$  about the y-axis will be

$$\bar{u}_{i,2} = B^{-1}(\gamma_2) B(\gamma_1) \bar{u}_{i,1}. \quad (18)$$

Thus:

$$\bar{u}_{i2} = \begin{bmatrix} -\sin\gamma_2 & \cos\gamma_2 \\ \cos\gamma_2 & \sin\gamma_2 \end{bmatrix} \begin{bmatrix} -\sin\gamma_1 & \cos\gamma_1 \\ \cos\gamma_1 & \sin\gamma_1 \end{bmatrix} u_{i1} \quad (19)$$

which gives:

$$\bar{u}_{i2} = \begin{bmatrix} \cos\gamma & -\sin\gamma \\ \sin\gamma & \cos\gamma \end{bmatrix} \bar{u}_{i1} \quad (20)$$

where  $\gamma = \gamma_2 - \gamma_1$ .

Additionally, the increment between the final and initial position of a leg  $\Delta\bar{u}_i = \bar{u}_{i2} - \bar{u}_{i1} = [\Delta x_i, \Delta z_i]^T$ , can be written as:

$$\Delta\bar{u}_i = \begin{bmatrix} \cos\gamma - 1 & -\sin\gamma \\ \sin\gamma & \cos\gamma - 1 \end{bmatrix} \bar{u}_{i1} \quad (21)$$

Finally, if the variation of  $\theta$  and  $\gamma$  are small the contribution of both angles for the incremental transform is:

$$\Delta\bar{v}_i = \Delta\bar{w}_i + \Delta\bar{u}_i = [\Delta x_i, \Delta y_i, \Delta z_{i\theta} + \Delta z_{i\gamma}]^T. \quad (22)$$

The vector-matrix equation relating incremental foot coordinate changes to initial foot coordinates in the body reference frame and body attitude is:

$$\begin{bmatrix} \Delta x_i \\ \Delta y_i \\ \Delta z_i \end{bmatrix} = \Delta C \begin{bmatrix} x_i \\ y_i \\ z_i \end{bmatrix}. \quad (23)$$

Where  $\Delta C$  is derived from Equations (11) and (21) as:

$$\begin{aligned} \Delta C &= \begin{bmatrix} \cos\gamma - 1 & 0 & -\sin\gamma \\ 0 & 0 & 0 \\ \sin\gamma & 0 & \cos\gamma - 1 \end{bmatrix} + \begin{bmatrix} 0 & 0 & 0 \\ 0 & \cos\theta - 1 & \sin\theta \\ 0 & -\sin\theta & \cos\theta - 1 \end{bmatrix} \\ &= \begin{bmatrix} \cos\gamma - 1 & 0 & -\sin\gamma \\ 0 & \cos\theta - 1 & \sin\theta \\ \sin\gamma & -\sin\theta & \cos\gamma + \cos\theta - 2 \end{bmatrix} \end{aligned} \quad (24)$$

which gives the incremental change in the leg position,  $[\Delta x, \Delta y, \Delta z]^T$ , to go from  $(\theta_1, \gamma_1)$  tilt to  $(\theta_2, \gamma_2)$ .

The final foot coordinate values are related to the initial foot coordinate values and body attitude by using absolute coordinate transforms. The absolute coordinate transform matrix is obtained by multiplying the two absolute transforms together, Equations (10) and (20), i.e.:

$$C = AB = \begin{bmatrix} \cos\gamma & 0 & -\sin\gamma \\ 0 & 1 & 0 \\ \sin\gamma & 0 & \cos\gamma \end{bmatrix} \begin{bmatrix} 1 & 0 & 0 \\ 0 & \cos\theta & \sin\theta \\ 0 & -\sin\theta & \cos\theta \end{bmatrix} \quad (25)$$

If the body is rotated by an angle  $\theta$  about the X-axis and an angle  $\gamma$  about the Y-axis of the initial coordinate system, the new foot location in the body coordinate frame will be:

$$\bar{x} = C\bar{x}_0$$

$$\bar{x} = \begin{bmatrix} \cos\gamma & \sin\theta\sin\gamma & -\cos\theta\sin\gamma \\ 0 & \cos\theta & \sin\theta \\ \sin\gamma & -\sin\theta\cos\gamma & \cos\theta\cos\gamma \end{bmatrix} \bar{x}_0 \quad (26)$$

where  $\bar{x}_0$  is the initial foot located coordinates and  $\bar{x}$  is the final foot location coordinates in the body reference frame.

To return to the level position the inverse of  $C$  is used:

$$\bar{x}_0 = \begin{bmatrix} \cos\gamma & 0 & \sin\gamma \\ \sin\theta\sin\gamma & \cos\theta & -\sin\theta\cos\gamma \\ -\cos\theta\sin\gamma & \sin\theta & \cos\theta\cos\gamma \end{bmatrix} \bar{x} \quad (27)$$

### 2.1.2 Deriving the Levelling Equations by Using Rotation Matrices

The change in link lengths and angle  $\alpha$  (see Figure 6) for each leg to bring the body to a desired tilt may be calculated by using rotation matrices.

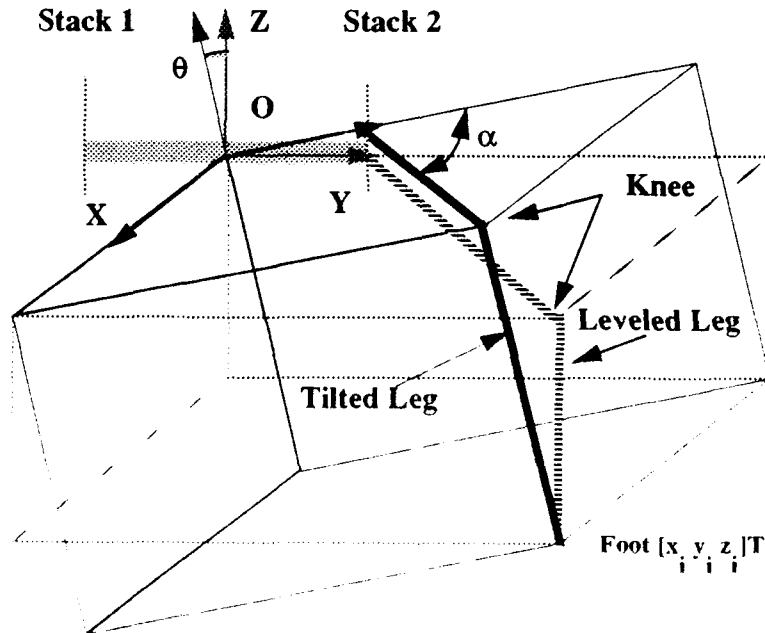


FIGURE 6. An Ambler leg in two configurations

As shown in Figure 6, the length of the vertical link is in both cases the z-coordinate of the foot in the body reference system, and the coordinates of the knee are  $[x_i \ y_i \ 0]^T$  where the foot position is  $[x_i \ y_i \ z_i]^T$ . The body reference system tilts with the machine (see the shaded arrows), such that the horizontal linkages are always in the XY plane in the body reference system. An equivalent leg is defined, as shown in Figure 7, such that the knee and the foot are in the same position as with the AMBLER leg and a hip is introduced. The foot coordinates in the body reference system,  $[x_i \ y_i \ z_i]^T$ , are the same as the link lengths of the Ambler-equivalent leg. This leg is used in simulations as opposed to the Ambler leg for clarity. The results hold equally for the Ambler leg itself.

To derive the equations of leveling, the body is rotated about the X-axis by an angle  $\theta$ . The new link lengths of the Ambler-equivalent leg, in the rotated body frame, are given by the coordinates of the foot, in the leveled body frame, when the leg is rotated by  $-\theta$ . Thus,

$$\bar{x} = Rot(X, -\theta)\bar{x}_0. \quad (28)$$

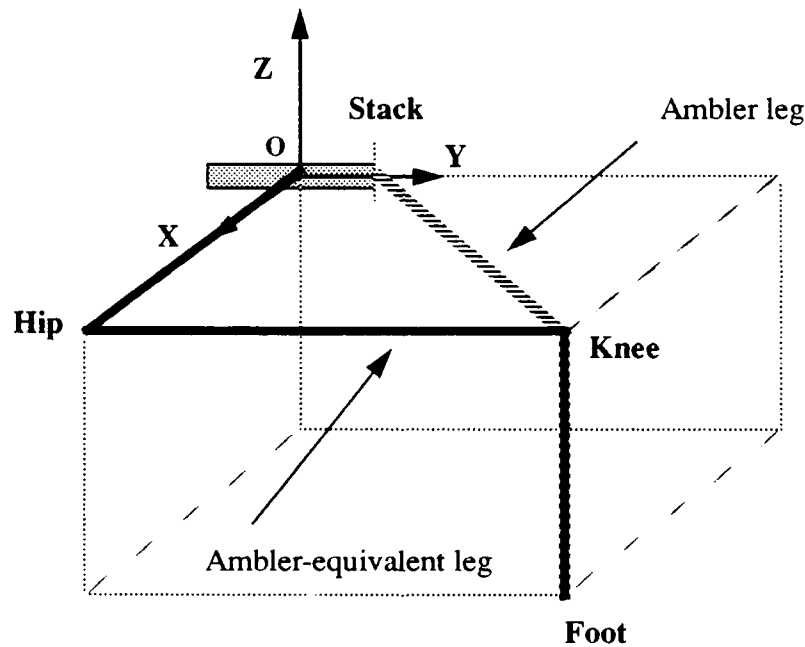


FIGURE 7. Diagram of the Ambler-equivalent leg

If the body is rotated by an angle  $\gamma$  about the Y-axis of the initial coordinate system, the new link lengths will be:

$$\bar{x} = Rot(Y, -\gamma)Rot(X, -\theta)\bar{x}_0 = \begin{bmatrix} \cos\gamma & \sin\theta\sin\gamma & -\cos\theta\sin\gamma \\ 0 & \cos\theta & \sin\theta \\ \sin\gamma & -\sin\theta\cos\gamma & \cos\theta\cos\gamma \end{bmatrix} \bar{x}_0. \quad (29)$$

Conversely, if the link lengths and the angles of the plane XY with the gravity vector are known, the body may be brought into the level position. Additionally, the rotation order is not

commutative. This has no significant effect for small angles such as the tilts that AMBLER will be allowed to make; therefore, this approximation is good enough for leveling the AMBLER.

If the foot position of leg  $i$  in a tilted configuration is  $[x_i \ y_i \ z_i]^T$ , then the knee position will be  $[x_i \ y_i \ 0]^T$ , and the hip position will be  $[x_i \ 0 \ 0]^T$ . To get these points in the leveled reference system, the inverse transformation matrix is used:

$$\bar{x}_i = (Rot(Y, -\gamma) Rot(X, -\theta))^{-1} \bar{x} = \begin{bmatrix} \cos\gamma & 0 & \sin\gamma \\ \sin\theta \sin\gamma & \cos\theta & -\sin\theta \cos\gamma \\ -\cos\theta \sin\gamma & \sin\theta & \cos\theta \cos\gamma \end{bmatrix} \bar{x}. \quad (30)$$

Equations (29) - (30) are equivalent to Equations (26) - (27), Therefore, the leveling equations derived by the methods described in these last two sections are equivalent.

## 2.2 Z-axes-leveling Methods

The previously-described method requires motion of all eighteen actuators; to do this all eighteen brakes must be released. If the body is leveled by only using the vertical joints, the brakes need to be released for only one third of the actuators. Thus, the latter method uses less "housekeeping" energy. As these devices have high power consumption and the AMBLER must be an efficient machine, several approaches to this kind of leveling were considered to find out the advantages and shortcomings of leveling by only using the Z-axes actuators.

### 2.2.1 Simple Z-axes-leveling Method

This leveling method is based on the kinematic approximations used by Klein [6]. While his work differs in that he generated velocity commands within the framework of active compliance, the small angle approximation that he uses is adopted, and only the vertical motions are used to level the body. This set of assumptions is widely used on other walking machines [3]-[5]. Referring to Figure 8, the angle  $\gamma$  is about the Y axis, and the angle  $\theta$  is about the X axis. To compensate for a change in  $\gamma$ , the change in the vertical extension of leg  $i$  is:

$$\Delta z_{Ri} = DR_i \sin\gamma. \quad (31)$$

Similarly, the change of length of the vertical axis for a change in  $\theta$  is given by:

$$\Delta z_{Pi} = -DP_i \sin\theta. \quad (32)$$

To effect both a change about  $x$  and  $y$  axes, these length changes are superimposed, i.e.:

$$\Delta z_i = DR_i \sin\gamma - DP_i \sin\theta \quad (33)$$

This method of leveling succeeds in bringing the body close to the desired inclination. This is, however, at the cost of body repositioning and possible foot slippage that will be analyzed in detail in the next section.

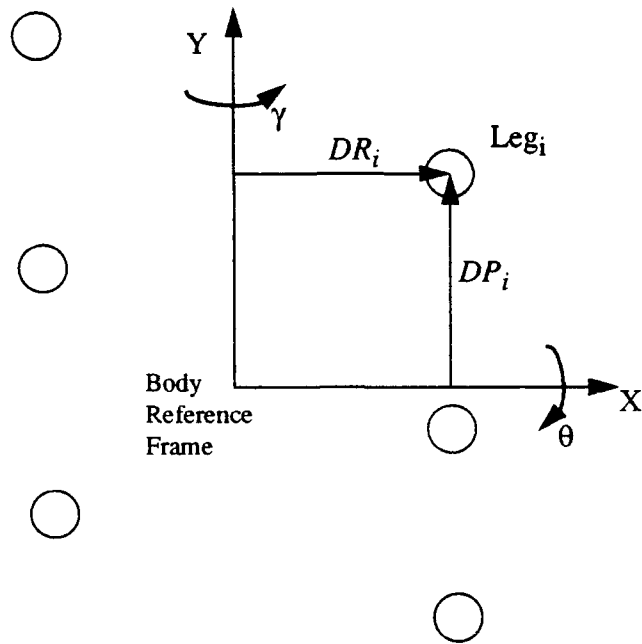


FIGURE 8. Rotations required to level the body

### 2.2.2 Z-axes-leveling Method from the All-axes-leveling Method

The vertical actuations commanded by the rotation matrix method derived for all axes may be used to level the body. The length changes commanded by this method differ slightly from the change given by Equation (33). This is because this method utilizes more kinematic information than the Simple Z-axes-leveling method. The transformation matrix for achieving this is then derived from Equation (29) as:

$$\bar{x} = \begin{bmatrix} 1 & 0 & 0 \\ 0 & 1 & 0 \\ \sin\gamma & -\sin\theta\cos\gamma & \cos\theta\cos\gamma \end{bmatrix} \bar{x}_0. \quad (34)$$

This method presents several shortcomings that can be summarized as: slight motion in the vertical plane while leveling, possible foot slippage, and the inconvenience of using this method for attitude control since the machine loses altitude during tilting maneuvers as shown in the third section of this report.

### 2.2.3 Isoaltitude Z-axes-leveling Method

A leveling method was then formulated with the constraint that the body frame moves only in the horizontal plane with a constant  $y$  coordinate value, as shown in Figure 9(a). If the origin of one coordinate system is translated to be coincident with the other, the two legs configurations are as shown in Figure 9(b). This is similar to the formulation shown in Section 2.1.1, but only the constraints that segments  $a_i$  and  $a_j$  do not change are used (see Figure 4). With these constraints,

the leg kinematics are defined by Equations (1) and (12) with the projections of the leg onto the planes YZ and ZX respectively.

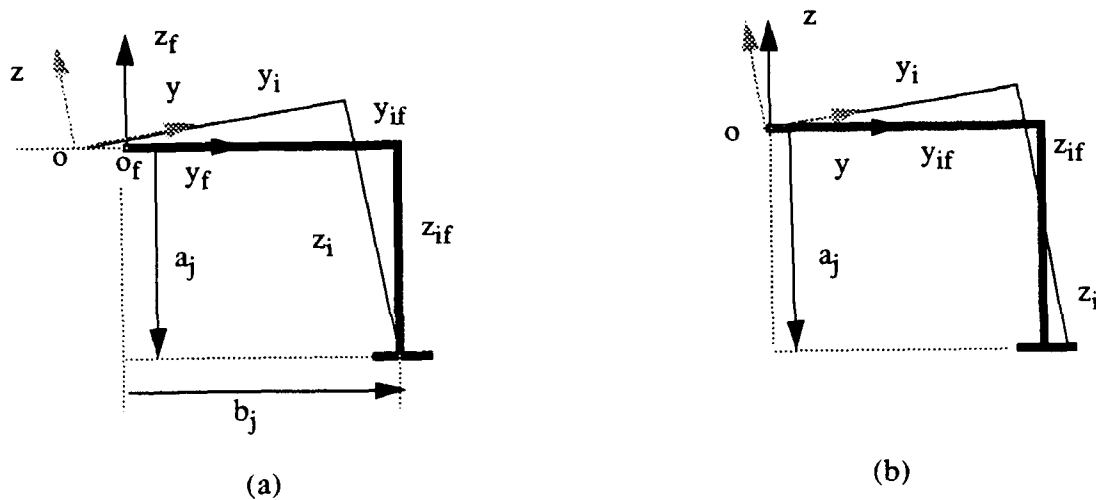


FIGURE 9. Motion of a leg for the Isoaltitude Z-axis-leveling method

If the tilt of the machine changes from  $(\theta_1, \gamma_1)$  to  $(\theta_2, \gamma_2)$ , using Equations (1) and (12) and considering that segments  $a_i$  and  $c_i$  and the horizontal coordinates  $x_i$  and  $y_i$  do not change, the equation for the projection onto the plane YZ is obtained:

$$y_i \sin \theta_1 + z_{1i} \cos \theta_1 = y_i \sin \theta_2 + z_{2i} \cos \theta_2 \quad (35)$$

and the incremental change in the  $z_i$  coordinate due to the contribution of  $\theta$  angle is:

$$\Delta z_{\theta_i} = z_{2i} - z_{1i} = \frac{z_{1i} (\cos \theta_1 - \cos \theta_2) + y_i (\sin \theta_1 - \sin \theta_2)}{\cos \theta_2} \quad (36)$$

Similarly, for the projection onto the plane XZ:

$$-x_i \sin \gamma_1 + z_{1i} \cos \gamma_1 = -x_i \sin \gamma_2 + z_{2i} \cos \gamma_2 \quad (37)$$

and the incremental change in the  $z$  coordinate due to the contribution of  $\gamma$  angle is:

$$\Delta z_{\gamma_i} = z_{2i} - z_{1i} = \frac{z_{1i} (\cos \gamma_1 - \cos \gamma_2) - x_i (\sin \gamma_1 - \sin \gamma_2)}{\cos \gamma_2} \quad (38)$$

Finally, the incremental change in  $z$  coordinates due to small rotations about  $x$  and  $y$  axes is found by combining Equation (36) and (38):

$$\Delta z_i = \Delta z_{\theta_i} + \Delta z_{\gamma_i}$$

$$= \left[ \begin{array}{c} \frac{\sin \gamma_1 - \sin \gamma_2}{\cos \gamma_2} \frac{\sin \theta_1 - \sin \theta_2}{\cos \theta_2} \left( \frac{\cos \theta_1}{\cos \theta_2} + \frac{\cos \gamma_1}{\cos \gamma_2} - 2 \right) \end{array} \right] \begin{bmatrix} x_i \\ y_i \\ z_{1i} \end{bmatrix}. \quad (39)$$

### 3. Kinematic Simulations

#### 3.1 All-axes-leveling Method

Simulation of the different methods of attitude control applied to the Ambler-equivalent model illustrates the leveling phenomena. The coordinates of the foot, knee and hip points of the Ambler-equivalent model are:

$$\begin{bmatrix} x \\ y \\ z \end{bmatrix}_{foot_i} = \begin{bmatrix} x_{i0} \\ y_{i0} \\ x_{i0} \end{bmatrix} \quad (40)$$

$$\begin{bmatrix} x \\ y \\ z \end{bmatrix}_{knee_i} = \mathfrak{R}^{-1}(\theta, \gamma) \begin{bmatrix} x_{i0} \\ y_{i0} \\ 0 \end{bmatrix} \quad (41)$$

$$\begin{bmatrix} x \\ y \\ z \end{bmatrix}_{hip_i} = \mathfrak{R}^{-1}(\theta, \gamma) \begin{bmatrix} x_{i0} \\ 0 \\ 0 \end{bmatrix} \quad (42)$$

where  $[x_{i0} \ y_{i0} \ z_{i0}]^T$  is the position of foot  $i$  in the body coordinate system and  $\mathfrak{R}$  is the transformation matrix defined in Equation (29).

The plots show that for different tilt angles and the same initial position, neither the feet nor the body frame moves, and the horizontal and vertical links in each leg maintain a right angle to one another. This can be seen in Figure 10 which contains a superposition of the Ambler-equivalent model at  $\theta = 5^\circ$  and  $\theta = 0^\circ$  with  $\gamma = 0^\circ$ . The initial positions of the feet are given in Table 1, which is the initial position for all examples shown in this report. These coordinates are given in the body reference system shown in Figure 10; therefore, this initial feet coordinate values are also the link lengths at level. For further clarification, the projection of the legs onto the plane XZ has also been made.

**TABLE 1.** Initial foot positions and link lengths at level for the Ambler-equivalent model

leg	x (cm)	y (cm)	z (cm)
0	100.	230.	-250.
1	120.	-240.	-250.
2	50.	270.	-200.
3	-50.	-260.	-250.
4	-100.	250.	-250.
5	-130.	-240.	-200.

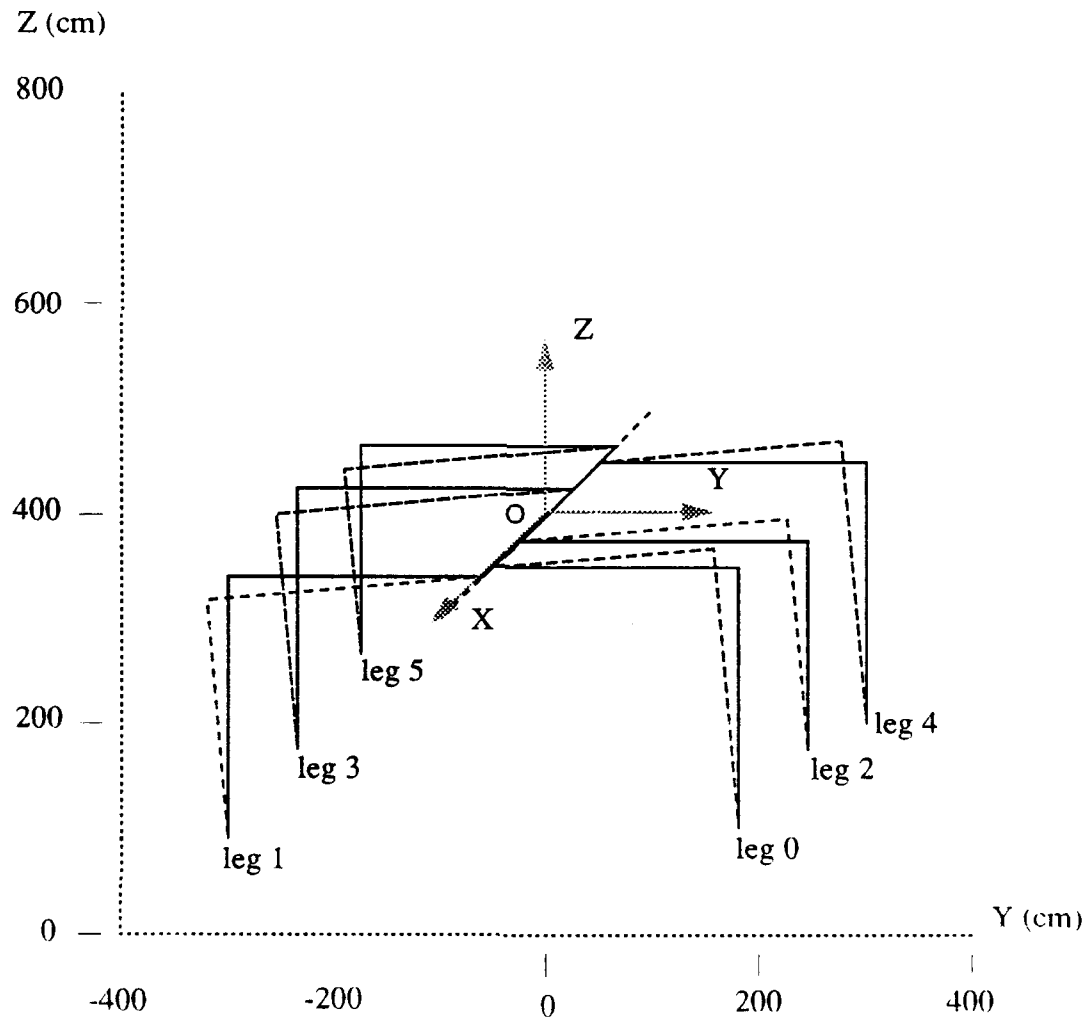


**FIGURE 10.** Superposition of the Ambler-equivalent model at  $\theta = 5^\circ$  and  $\theta = 0^\circ$  for  $\gamma = 0^\circ$

Following, there are several plots for different tilt angles and the same initial position for each foot. The constraint that the links maintain right angles is shown on the plane YZ for variations of  $\theta$ , and on the plane XZ for variations of  $\gamma$  (see Figures 11 - 13). The link lengths at tilt and the increments required to level the body are given in Tables 2 - 4 for each case.

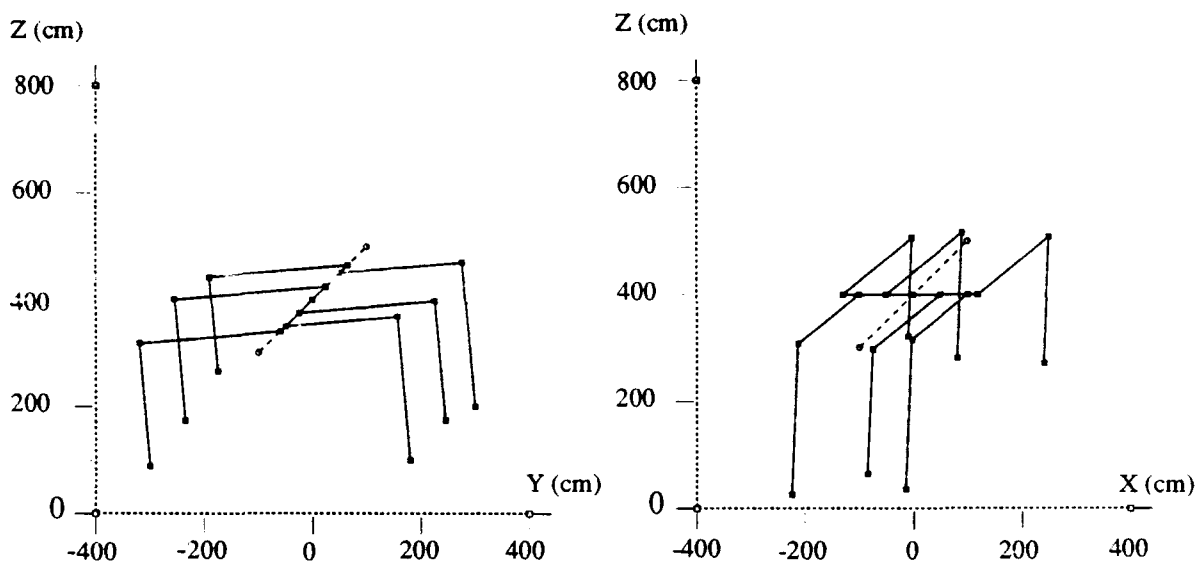


FIGURE 11. Ambler-equivalent model at  $\theta = 5^\circ$  and  $\gamma = 0^\circ$

TABLE 2. Link lengths at an initial tilt of  $\theta = 5^\circ$  and  $\gamma = 0^\circ$ , and link increments to level the body;

leg	x (cm)	y (cm)	z (cm)	d2 (cm)	inc x (cm)	inc y (cm)	inc z (cm)
0	100.	207.3	-269.0	149.2	0.	22.6	19.0
1	120.	-260.8	-228.1	203.5	0.	20.8	-21.8
2	50.	251.5	-222.7	162.8	0.	18.4	22.7
3	-50.	-280.8	-226.3	190.9	0.	20.8	-23.6
4	-100.	227.2	-270.8	164.5	0.	22.7	20.8
5	-130.	-256.5	-178.3	206.1	0.	16.5	-21.6

The legs of the Ambler-equivalent model in this first example are in parallel YZ planes. Referring to the plane YZ in Figure 11, the horizontal and vertical links maintain perpendicularity. Link lengths at the tilt position and the increments in each link needed to level the body are shown in Table 2. In this case, the x-coordinate values do not change because the rotation is about the x-

axis. The length of the horizontal link,  $d_2$ , (see Figure 1) for each leg is used to determine if the machine is within its mechanical limits. This value must be between 106 and 234 cm.

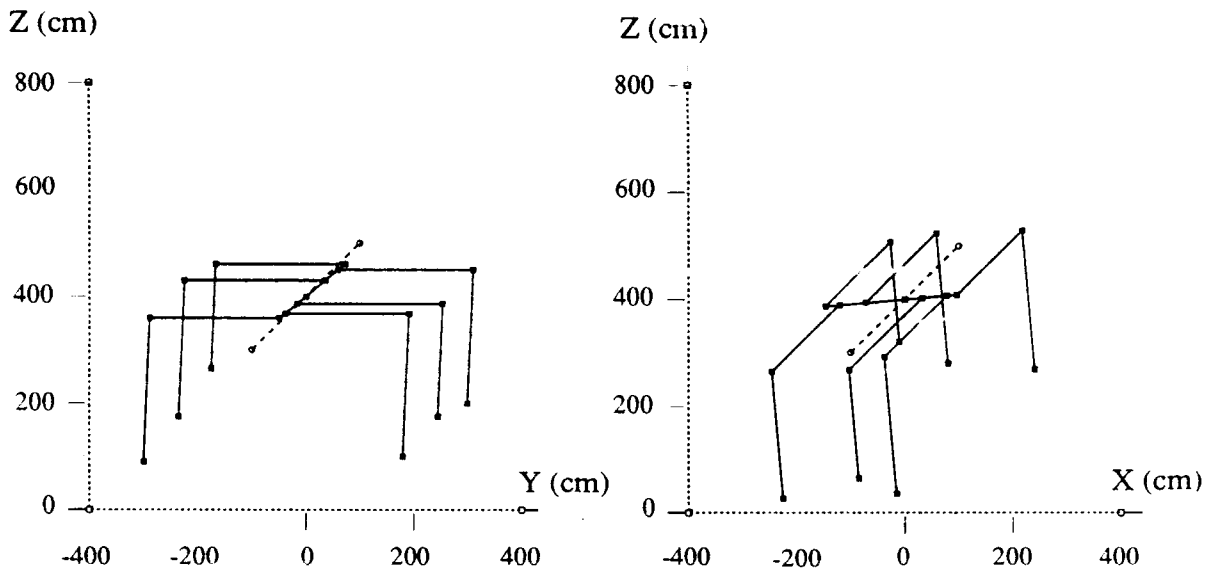


FIGURE 12. Ambler-equivalent model at  $\theta = 0^\circ$  and  $\gamma = -5^\circ$

TABLE 3. Link lengths at an initial tilt of  $\theta = 0^\circ$  and  $\gamma = -5$ , and link increments to level the body

leg	x (cm)	y (cm)	z (cm)	d2 (cm)	inc x (cm)	inc y (cm)	inc z (cm)
0	77.8	230.	-257.7	154.5	22.1	0.	7.7
1	97.7	-240.	-259.5	173.6	22.2	0.	9.5
2	32.3	270.	-203.5	176.4	17.6	0.	3.5
3	-71.5	-260.	-244.6	178.4	21.5	0.	-5.3
4	-121.4	250.	-240.3	195.6	21.4	0.	-9.6
5	-146.9	-240.	-187.9	205.3	16.9	0.	-12.0

Figure 13 shows the pose of the Ambler-equivalent model when the rotation about the y axis is -5 degrees. In this case, the perpendicularity is observed between the links by looking at plane XZ. In this case, the y coordinate does not change because the rotation is about y-axis.

A change in all coordinates is required to level the body from an initial tilt of  $\theta = 5^\circ$  and  $\gamma = -5^\circ$ , (see Figure 13 and Table 4). In this case the perpendicularity between links cannot be observed from the perspective of the XZ or YZ planes.

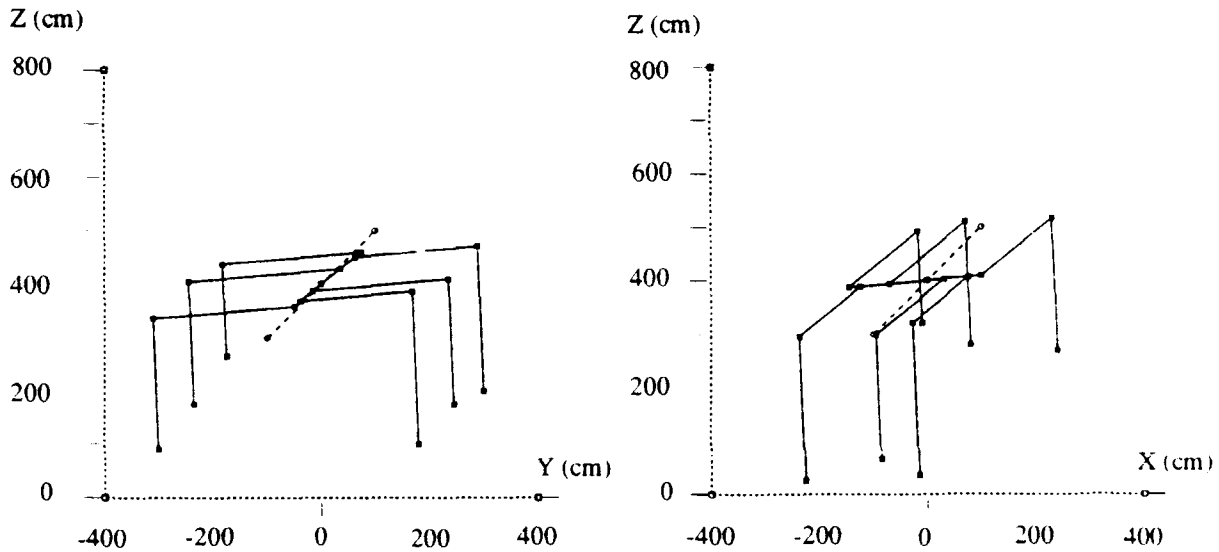


FIGURE 13. Ambler-equivalent model at  $\theta = 5^\circ$  and  $\gamma = -5^\circ$

TABLE 4. Link lengths at an initial tilt of  $\theta = 5^\circ$  and  $\gamma = -5^\circ$ , and link increments to level the body

leg	x (cm)	y (cm)	z (cm)	d2 (cm)	inc x (cm)	inc y (cm)	inc z (cm)
0	76.1	207.3	-276.7	134.4	23.8	22.6	26.7
1	99.6	-260.8	-237.7	192.2	20.3	20.8	-12.2
2	30.3	251.5	-226.2	157.9	19.6	18.4	26.2
3	-69.5	-280.8	-221.1	196.9	19.5	20.8	-28.8
4	-123.2	227.2	-261.0	179.6	23.2	22.7	11.0
5	-145.0	-256.5	-166.3	215.9	15.0	16.5	-33.6

Figures 14-16 show how the link lengths have to change, as a function of the tilt, to level the body from an initial attitude of  $\theta = 5^\circ$  and  $\gamma = -5^\circ$ . These functions are quasi-linear, as expected, and show how the coordinates change for different initial tilts.

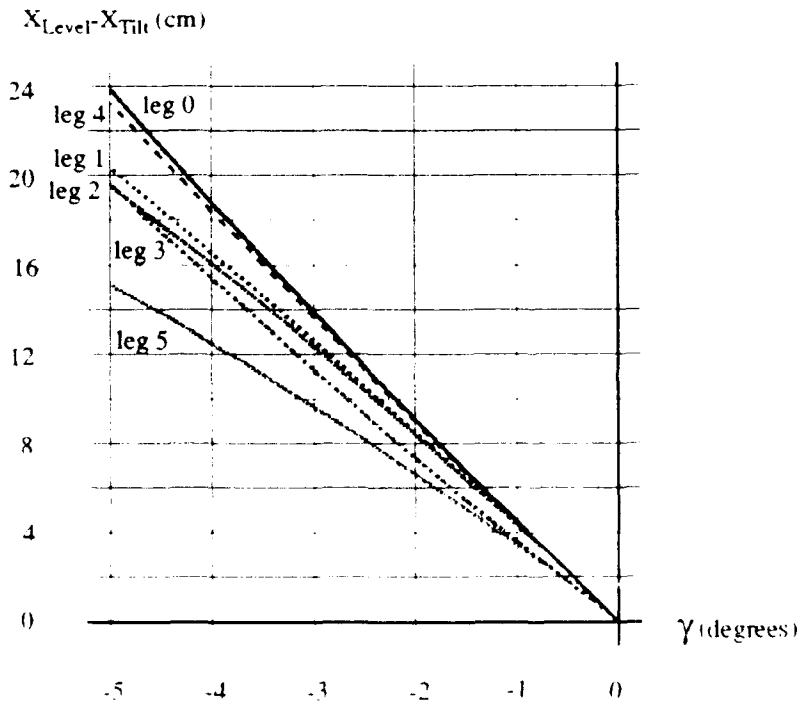
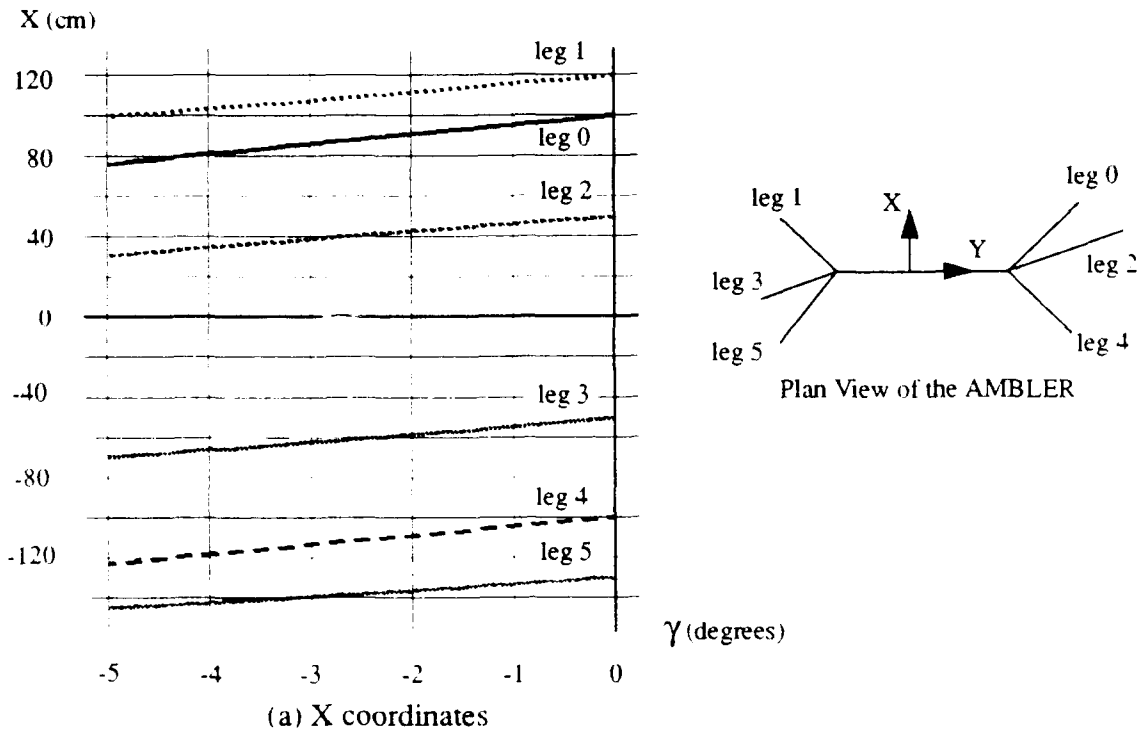
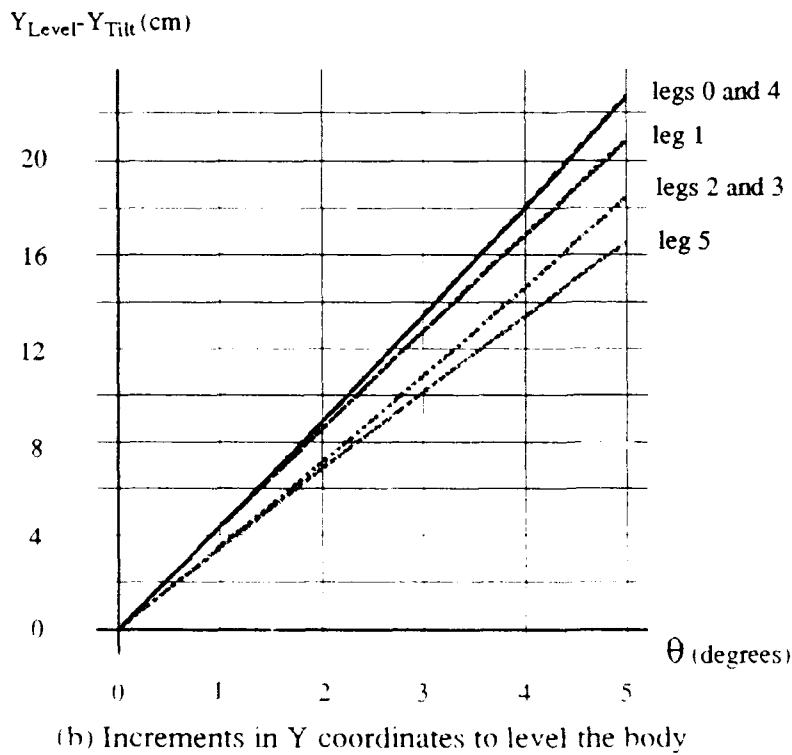
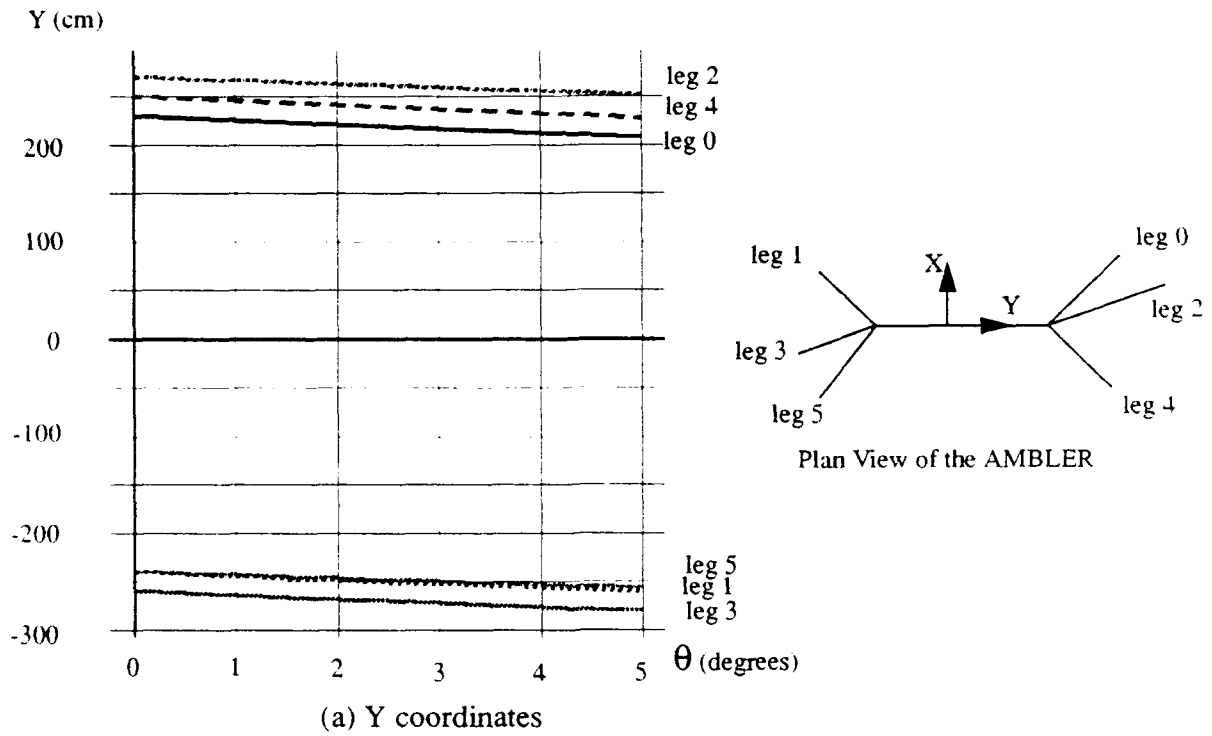


FIGURE 14. The X coordinates and their incremental changes during leveling



**FIGURE 15.** The Y coordinates and their incremental changes during leveling

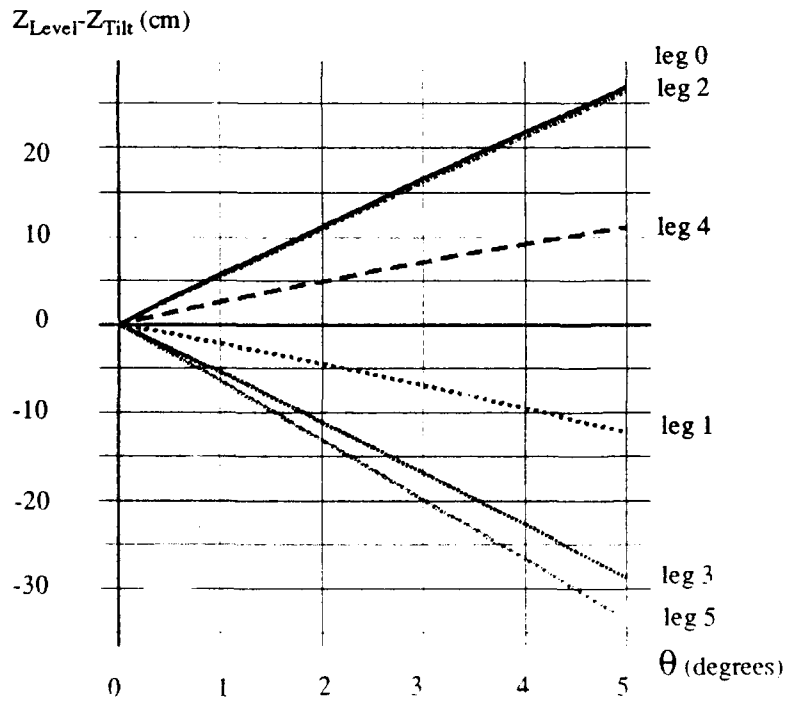
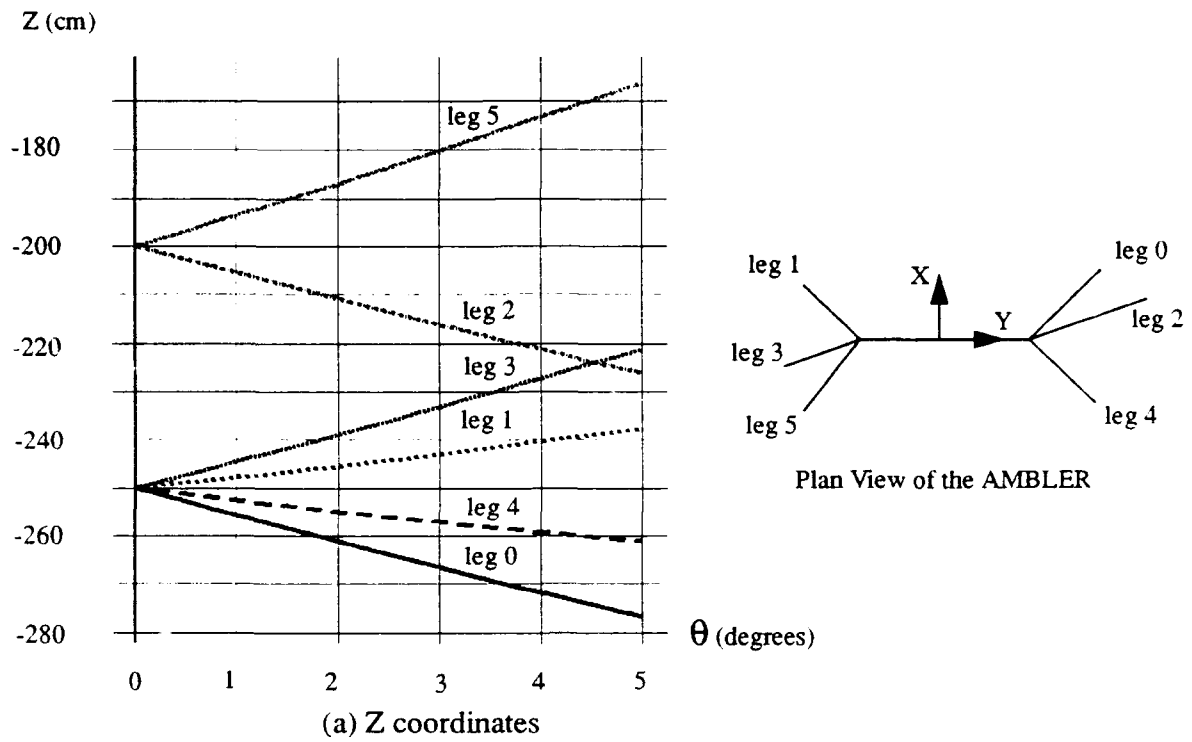


FIGURE 16. The Z coordinates and their incremental changes during leveling

### 3.2 Z-axes-leveling Method

When using all axes to level the body, the horizontal links of the AMBLER have to change about 20 cm during a leveling maneuver for rolls and pitches of  $5^\circ$  (see Figure 14-15). The body frame, however, does not move, since the horizontal links shorten by about this amount on one stack, and extend by a similar amount on the other. This implies that in the Z-axes-leveling method, in which the horizontal links do not change, the body frame should move significantly. To observe this phenomenon, the trajectory of a leg is simulated for the different Z-axes leveling methods (Figures 17-23).

#### 3.2.1 Simple Z-axes-leveling Method

Figure 17 shows the movement of the body frame, under the assumption that the leg shown (leg 1 in our example) does not slip, for a variation of the tilt from  $\theta = -20^\circ$  to  $\theta = 0^\circ$ . Such a big angle has been chosen to magnify the phenomena that arise with this leveling method. The body frame also moves in the vertical plane; therefore, work must be done against gravity when bringing the machine to a level position.

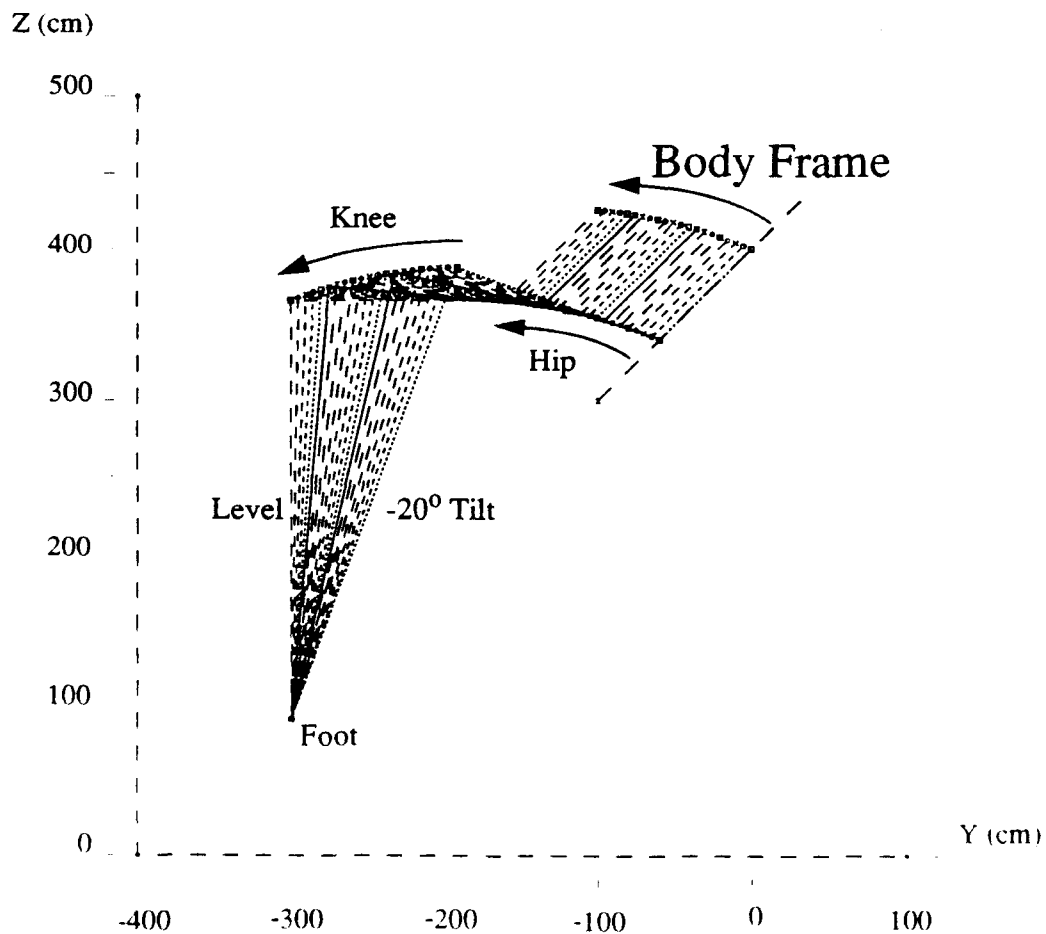
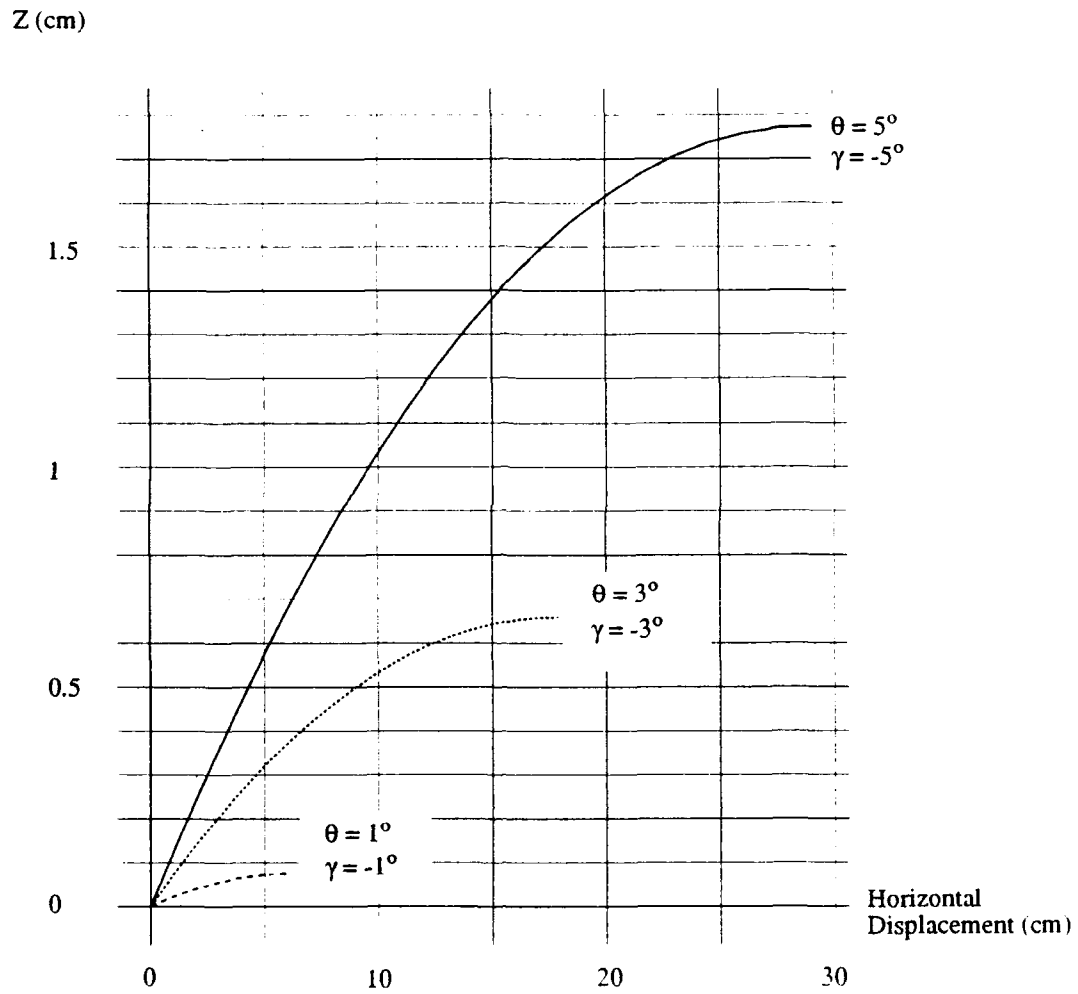


FIGURE 17. Displacement of the body frame, knee, and hip when using the Simple Z-axes method

The vertical and horizontal displacements required to level the body from different initial tilts are shown in Figure 18. The body frame translates in the horizontal plane by about 30 cm and rises by about 1.9 cm for an initial tilt of  $\theta = 5^\circ$  and  $\gamma = -5^\circ$ .



**FIGURE 18.** Displacement of the body frame for different initial tilts when using the Simple Z-axes-leveling method

### 3.2.2 Z-axes-leveling Method from the All-axes-leveling Method

Figure 19 shows the motion of the body frame under the same conditions as the Simple Z-axes-leveling method. The main difference with the previous method is that the body frame at the end of the motion is in the same horizontal plane as the start. However, it follows an arc, so this method also raises the body by a smaller amount than the previous one. Figure 20 shows the horizontal and vertical displacements when leveling the body from different initial tilts. The largest amount that the body raises is close to 1 cm for an initial tilt of  $\theta = 5^\circ$  and  $\gamma = -5^\circ$ . The magnitude of this amount depends on the AMBLER position; for example, for an initial tilt of  $\theta = -5^\circ$  and  $\gamma = -5^\circ$ , the maximum lift of the body frame is 1.05 cm. Thus, for the maximum tilt allowed in the AMBLER, the peak amount the body frame displaces by is about 1 cm when leveling the body.

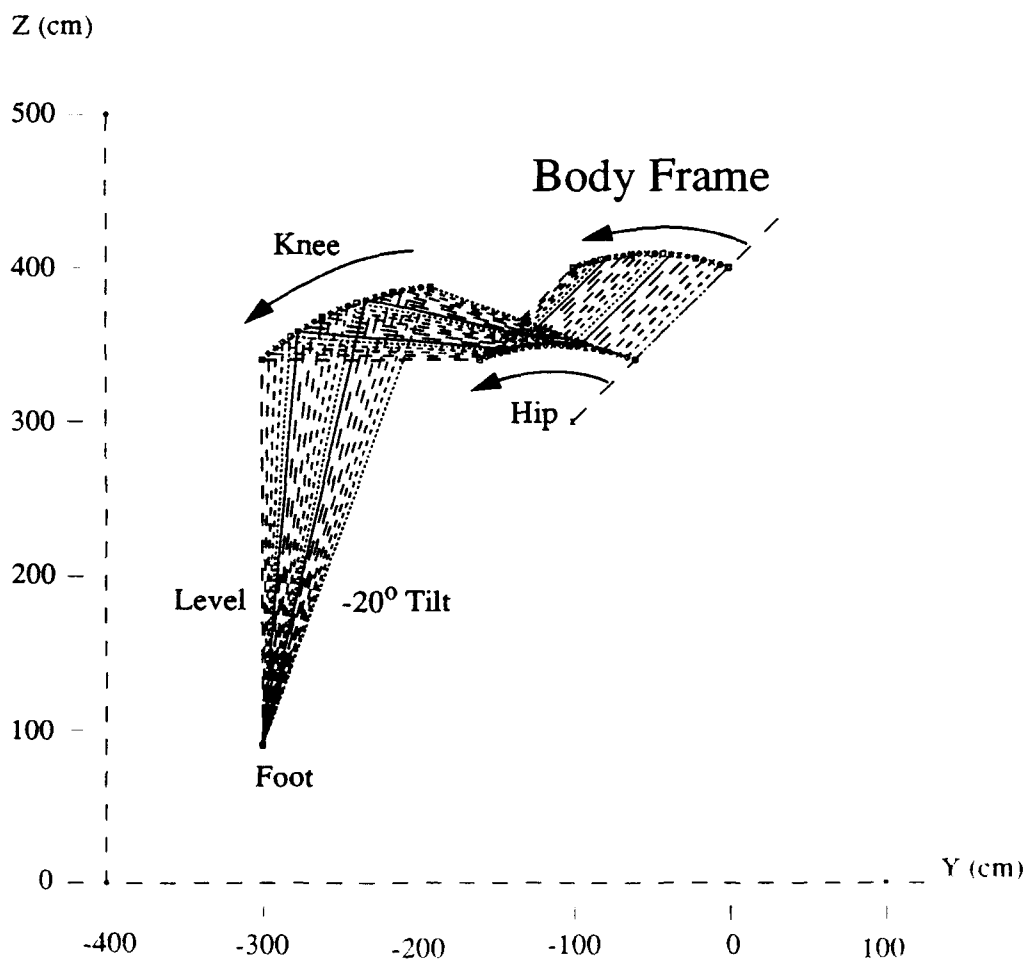


**FIGURE 19.** Displacement of the body frame, knee, and hip when using the Z-axes-leveling method from the All-axes leveling method

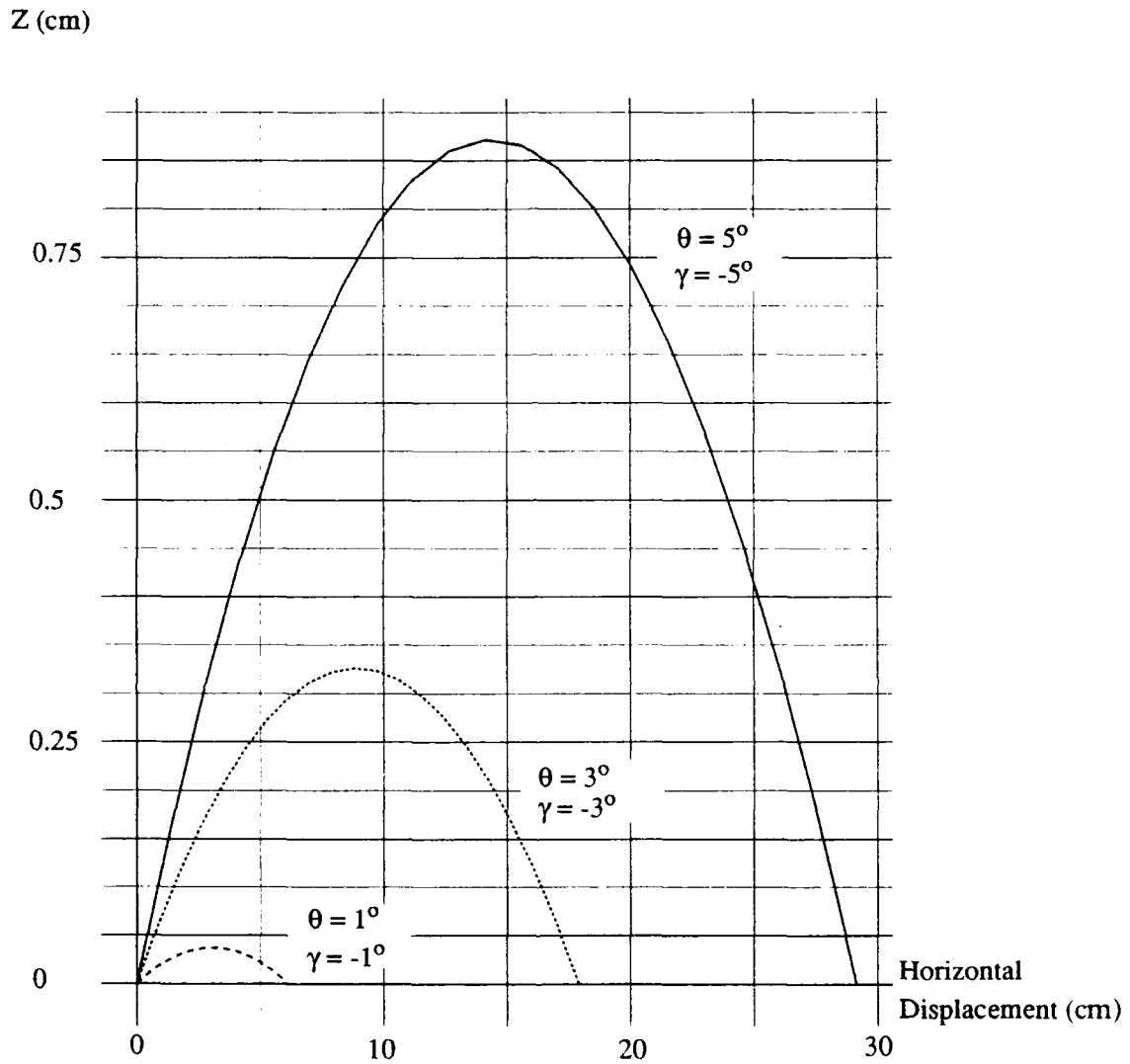


**FIGURE 20.** Displacement of the body frame for different initial tilts when using the Z-axis-leveling method from the All-axes-leveling method

This method works well to bring the body to level, but it has a severe shortcoming as shown in Figure 21. The leg in this figure is first shown in a level position. It then undergoes a tilt, and the body frame drops. It does not regain this height when the leg re-levels. Each time the body is tilted it loses altitude.

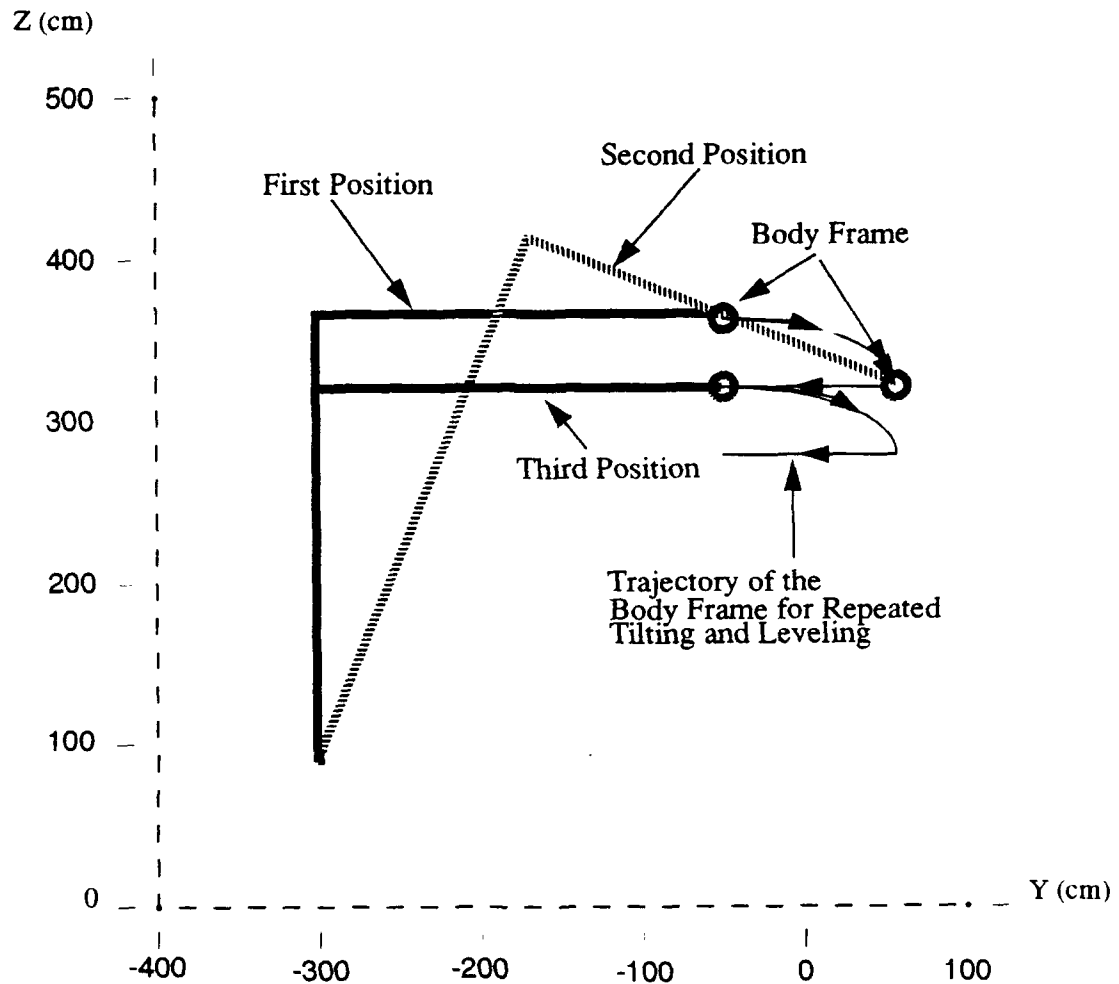


**FIGURE 21.** A sequence of tilting and leveling using the Z-axes-leveling method from the All-axes-leveling method

Therefore, this method is more convenient for leveling than the Simple Z-axes-leveling method because it keeps the body in the same plane, but it is not adequate for attitude control because the machine drops down whenever it is commanded to achieve non-zero tilts.

### 3.2.3 Isoaltitude Z-axes-leveling Method

Application of the Isoaltitude Z-axes-leveling equations is depicted in Figure 22. This figure shows the displacement of the body frame for a tilt of  $-20^\circ$  about the  $x$  axis. With this method, the motion of the body frame is constrained to the horizontal plane.

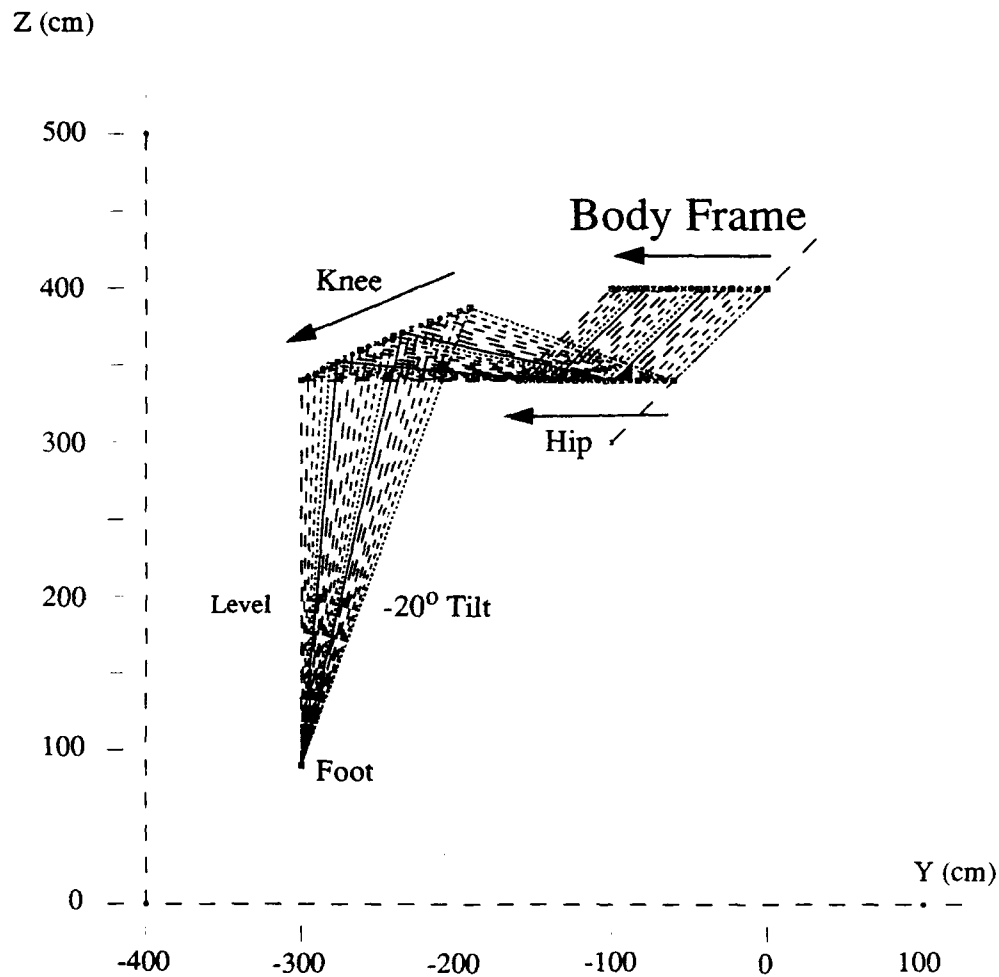
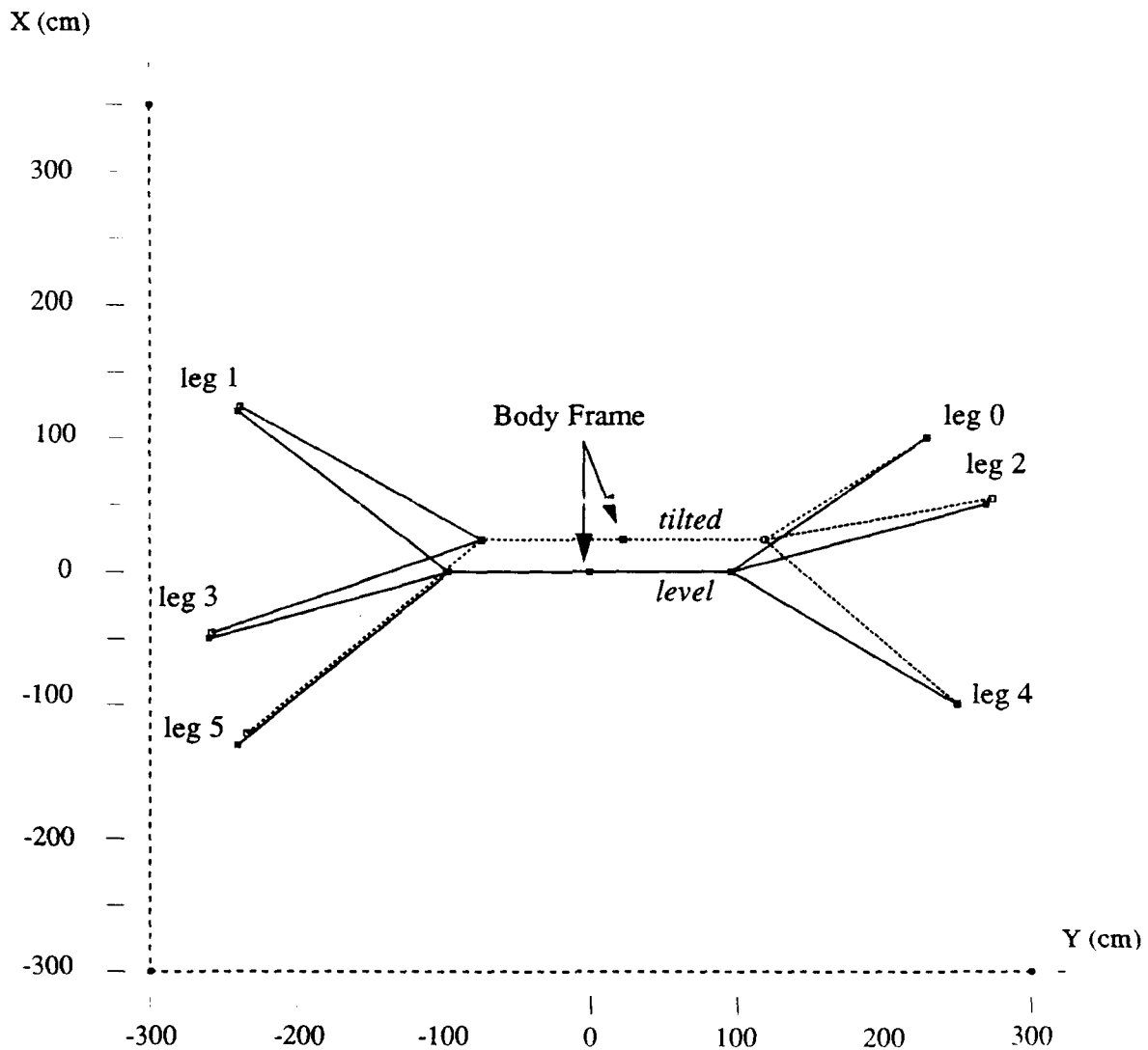


FIGURE 22. Displacement of the body frame, knee, and hip when leveling using the Isoaltitude Z-axis-leveling method

### 3.2.4 Foot Slippage

Figures 17-20 and 22 show how the body frame moves under the assumption that one foot does not slip and links and joints are rigid. This implies that all other feet will slip. To illustrate the foot slippage, a plan view of the Ambler-equivalent model is shown before and after leveling in Figure 23. The dotted line represents the tilted configuration, and the solid line the level configuration. In this example it is assumed that the closest leg to the body frame does not move. The figure shows the plan view of the machine and the data are given in Table 5. This table contains the link lengths at tilt, the increments required to level the body using the All-axes-leveling methods, the slippage of the feet, and the motion of the body frame. For this example, the

largest foot slippage is about 11 cm for leg 5 and the body frame moves by about 33 cm in the horizontal plane.



**FIGURE 23.** Plan view of the AMBLER at level (solid line) and at a tilt (dotted line) of  $\theta = 5^\circ$  and  $\gamma = -5^\circ$

This plot or the plane XY and the values of Table 5 are the same for all Z-axes-leveling methods because the only difference between these methods are on the Z-axis values.

**TABLE 5.** Data to level the body from an initial tilt of  $\theta = 5^\circ$  and  $\gamma = -5^\circ$

LINK LENGTHS AT TILT			
leg	x(cm)	y(cm)	z(cm)
0	76.1	207.3	-276.7
1	99.6	-260.8	-237.7
2	30.3	251.5	-226.2
3	-69.5	-280.8	-221.1
4	-123.2	227.2	-261.0
5	-145.0	-256.5	-166.3

INCREMENTS IN LINK LENGTHS FOR LEVELING			
leg	inc x(cm)	inc y(cm)	inc z(cm)
0	-23.8	22.6	26.7
1	-20.3	20.8	-12.2
2	-19.6	18.4	26.2
3	-19.5	20.8	-28.8
4	-23.2	22.7	11.0
5	-15.0	16.5	-33.6

FOOT SLIPPAGE IF ONLY THE Z-AXES ARE USED FOR LEVELING			
leg	Foot slippage in		Total foot slippage (cm)
	x-axis (cm)	y-axis (cm)	
0 <sup>2</sup>	0.0	0.0	0.0
1	3.4	1.7	3.9
2	4.2	4.2	5.9
3	4.2	1.8	4.6
4	0.6	0.0	0.6
5	8.7	6.1	10.7

DISPLACEMENT OF THE BODY FRAME IF ONLY Z-AXES ARE USED TO LEVEL ROBOT		
Displacement in x-axis (cm)	Displacement in y-axis (cm)	Total Displacement (cm)
23.8	22.6	32.8

<sup>2</sup> This is the closest leg to the center of the body. It is assumed that this leg does not move and all others slip.

By performing simulations, it became apparent that the slippage depends on the difference in elevation between feet. Thus, the maximum foot slippage was calculated when the non-slipping leg, leg 0, is at different heights relative to the other feet. For the example used in this document ( $x$  and  $y$  coordinates defined in Table 1, and the foot at  $-600$  cm for legs 1 to 5) the maximum foot slippage occurred with leg 5. Table 6 shows how much the slippage changes for varying the elevation of the non-slipping leg, as depicted in Figure 24. In this example, the body frame is  $600$  cm above feet 1 through 5. The worst slippage occurs when leg 0 has the highest foothold. In this instance, the theoretical slippage is about  $30$  cm and the question is whether the flexibility of the machine absorbs this variation or not. If not, the All-axes-leveling method should be used for leveling in very rough terrain or slopes. Otherwise, any Z-axes-leveling method could be used for leveling, noting that the Isoaltitude method gives the best performance.

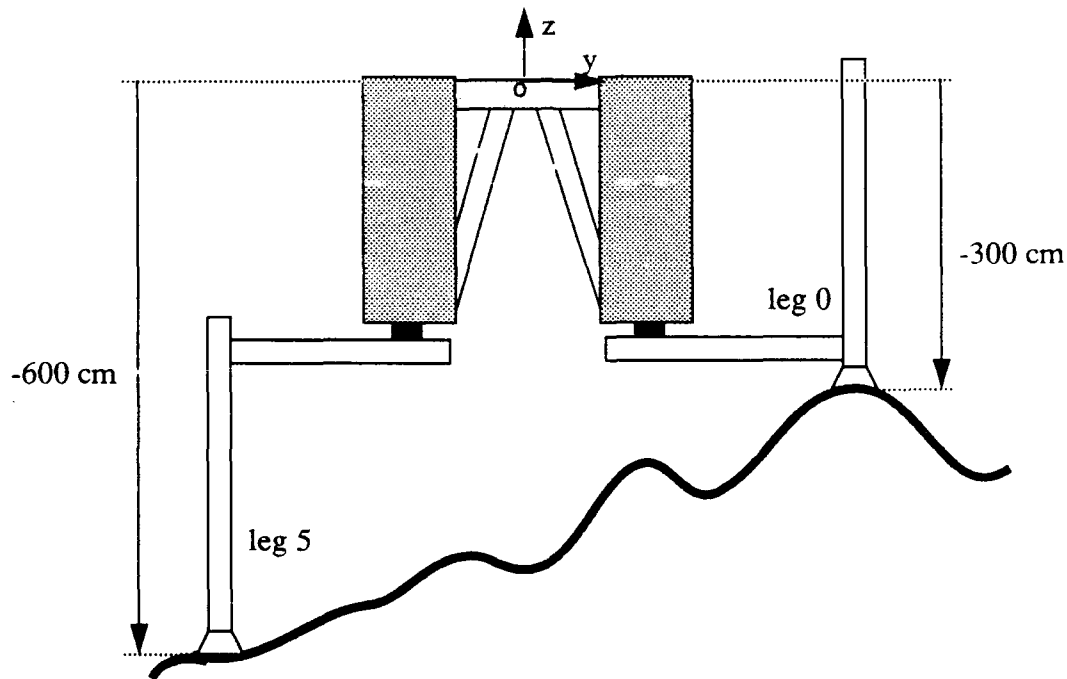


FIGURE 24. Maximum difference between leg extensions

TABLE 6. Foot slippage for leg 5 under variations of the extension on leg 0

Extension on leg 0 (cm)	Slippage on foot 5 (cm)
-600.	4.7
-500.	8.1
-400.	20.2
-300.	32.5

## 4. Implementation of Leveling Control on the AMBLER

The four leveling methods have been simulated, then implemented on the AMBLER. Measurements of the attitude and power consumption during leveling maneuvers were taken for comparison of the methods. These methods worked as expected although implementation revealed some undesirable features of the inclinometer sensors that will be discussed.

### 4.1 All-axes-leveling Method

The All-axes-leveling method was introduced in Section 2.1 to keep the body frame from translating. This formulation may be easily modified such that any arbitrary point does not translate, by substituting this location for the body frame in our formulation. In this section leveling without translation will be considered for two locations: (a) the body frame on the top of the machine, and (b) the body frame closer to the center of gravity of the machine (1.23 meters below the top of the machine). For the first case the motion of the body, as indicated by the inclinometers, is very smooth, and for the second case (see Figure 25), some spikes in the inclinometer readings appeared at the beginning and at the end of the motion. However, the motion was smooth in both cases.

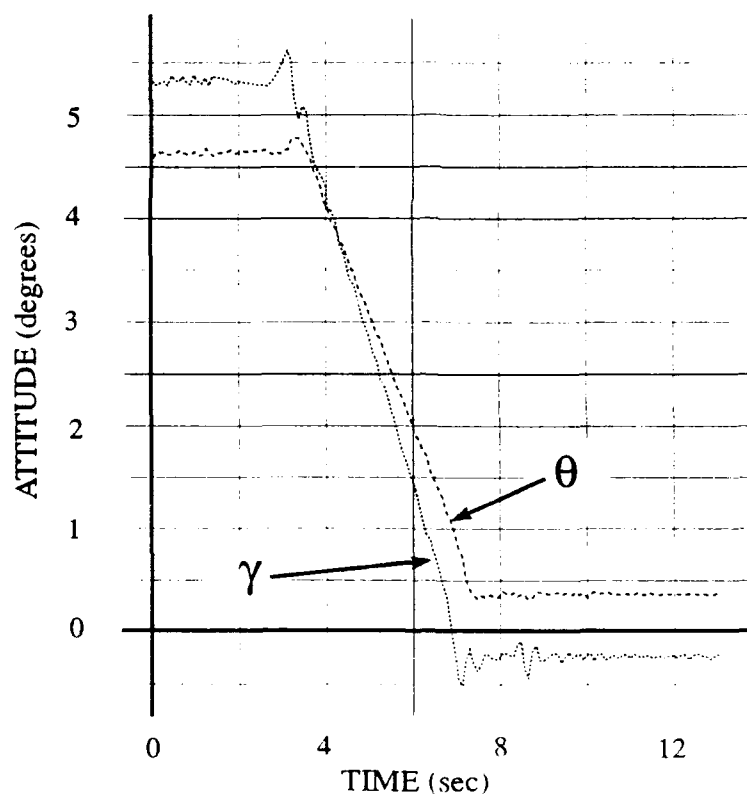


FIGURE 25. Attitude change during leveling for the All-axes-leveling method

These spikes are due to the behavior of the inclinometers. They are based on an oil-damped pendulum, and consequently they are sensitive to linear accelerations. Thus, the translational motion of the body interferes with the tilt readings and some problems can arise when using the inclinometers in a dynamic situation. One such situation is when support failures occur. The

reactive leveling algorithm [10] utilizes attitude sensors in the control loop. With terrain failure experiments, the AMBLER falls about half a meter in a very small time and a very large spike is generated by the inclinometers. This indicates a false tilt opposite to the actual tilt. Therefore the machine first tries to correct its attitude in the wrong direction if the inclinometers are used when controlling body attitude.

In case (a) the body frame is closer to the inclinometer position than in case (b); therefore, when the machine rotates, the linear acceleration of the inclinometers is smaller and the false spikes have smaller magnitudes.

During the experiments with the All-axes-leveling method, an inherent problem was detected because of the joint motion limitations of the horizontal links. As they are shorter than the vertical links, there are many poses from which it is not possible to achieve leveling due to joint motion limit constraints. The power consumption for this method is too high for two reasons. Releasing all brakes requires extra energy expenditure, and it also is necessary to drive the friction on eighteen actuators instead of just six of them (see Figures 29 - 30).

## 4.2 Z-axes-leveling Methods

The Simple Z-axes-leveling method moves the body frame as found in simulations (see Figure 17), so there is an initial displacement of the body that is registered as a spike, which is bigger than the spikes in the previous method (see Figure 26). The time to level the body is approximately the same as the time required in the All-axes-leveling method (the speed in vertical links was set at 0.07 m/sec in both cases), and the power consumption is much lower (see Figures 29 - 30 and Table 7).

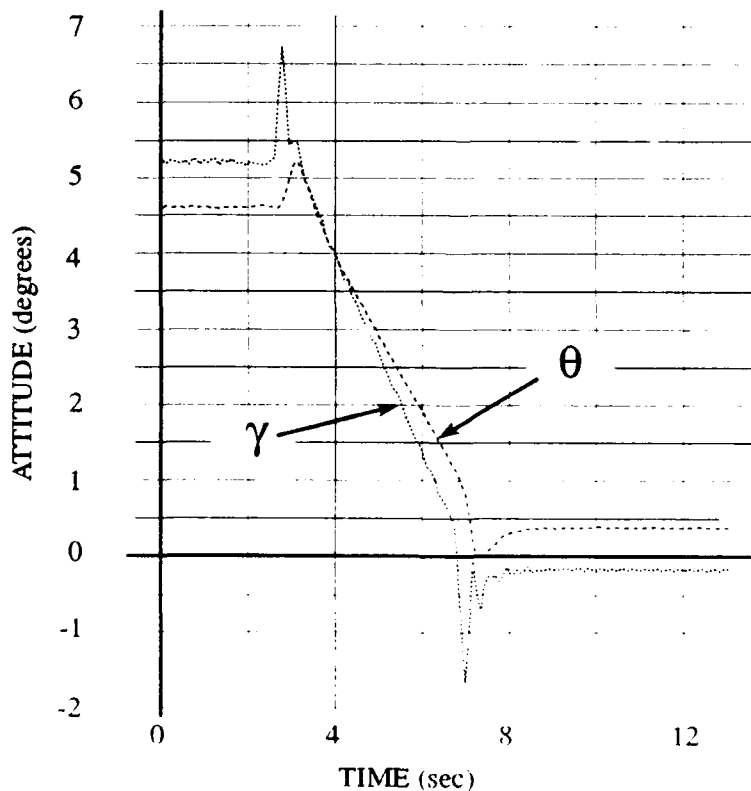
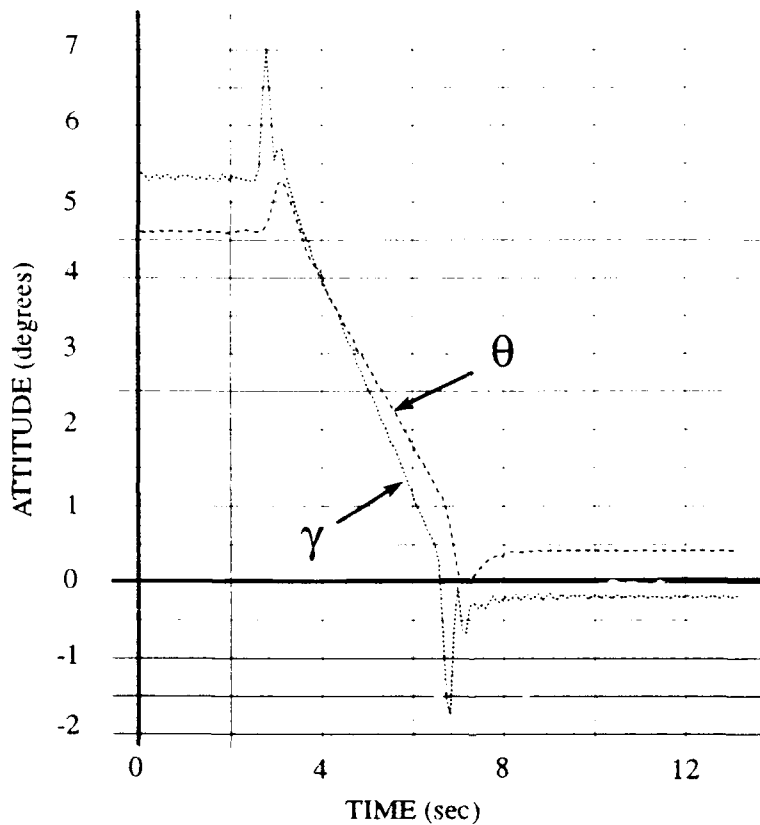


FIGURE 26. Attitude change during leveling for the Simple Z-axes-leveling method

The slippage of feet was expected but not detected in most cases. This is probably due to the flexibility of the AMBLER structure. Some of the displacement in feet is absorbed by flexion in legs and the frame of the body. However, when feet were at dissimilar elevation foot slippage did occur.

The Z-axes-leveling method from the All-axes-leveling method and the Isoaltitude leveling method work in a very similar way to the Simple Z-axes-leveling method. The leveling is achieved with practically no difference (compare Figures 26 and 27). The power consumption is somewhat lower; this probably occurs because the body rises less than with the Simple Z-axes method (see Figures 29 - 30 and Table 7).



**FIGURE 27.** Attitude change during leveling for the Z-axes-leveling method from the All-axes-leveling method and the Isoaltitude Z-axes-leveling methods

Theoretically, the Z-axes-leveling method from the All-axes-leveling method should consume more power than the Isoaltitude method, as the body is lifted in the vertical plane; however, the difference is so marginal that it is on the order of noise observed by the power meter.

### 4.3 Power Consumption Measurements

The power consumption measurements were taken using a power meter connected through an analog link to the control computer. The data were taken approximately at 12 Hz, and is corrupted

by noise, which arises from the PWM amplifiers. A digital filter was employed to get smoother curves.

Figure 28 shows the quality of the data collected for a leveling using the All-axes-leveling method. The dashed line shows the raw data from the power meter and the solid line shows the data after the application of a median filter which takes the median value of 20 consecutive points.

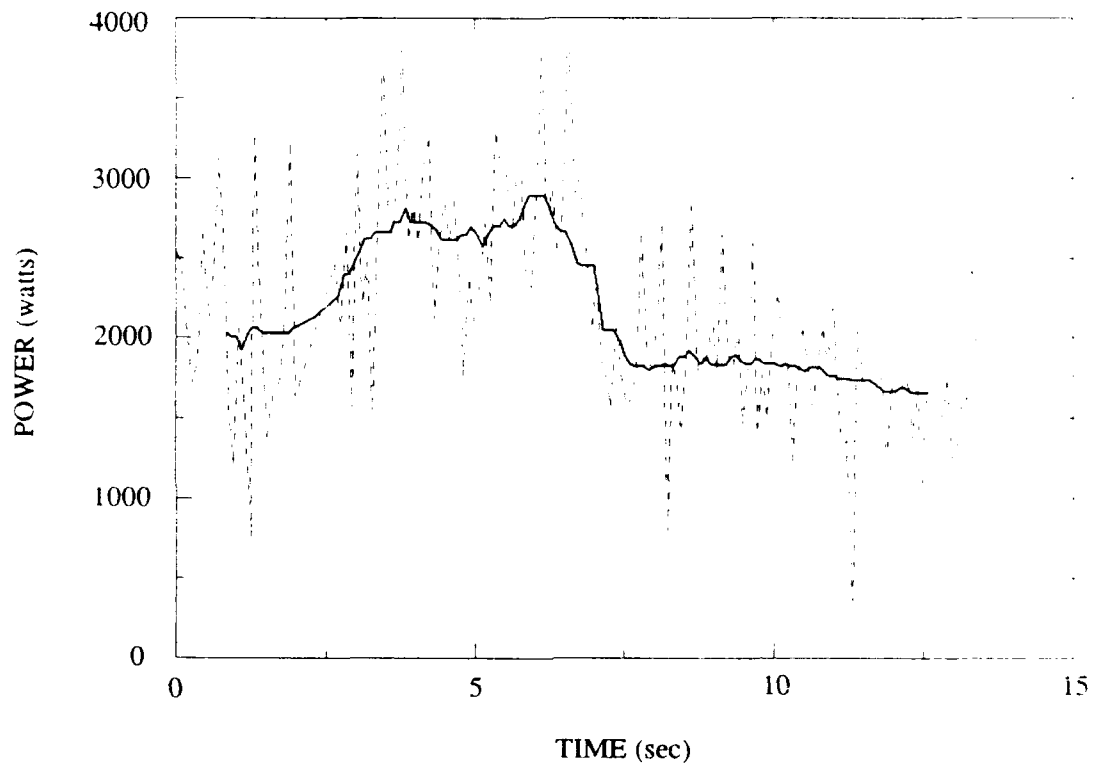


**FIGURE 28.** Raw data (dashed line) and filtered data (solid line) for a leveling using the All-axes-leveling method

The next two figures are plots showing the power consumption for each leveling method under different poses and attitudes. They show the results for leveling the body from an initial tilt of about 5 and 7 degrees respectively (comprised of equal rolls and pitches of 3 and 5 degrees respectively). The All-axes-leveling method requires much more power than the Z-axis methods, which were comparable. To augment these plots, Table 7 shows the readings on the power meter display during the experiments.

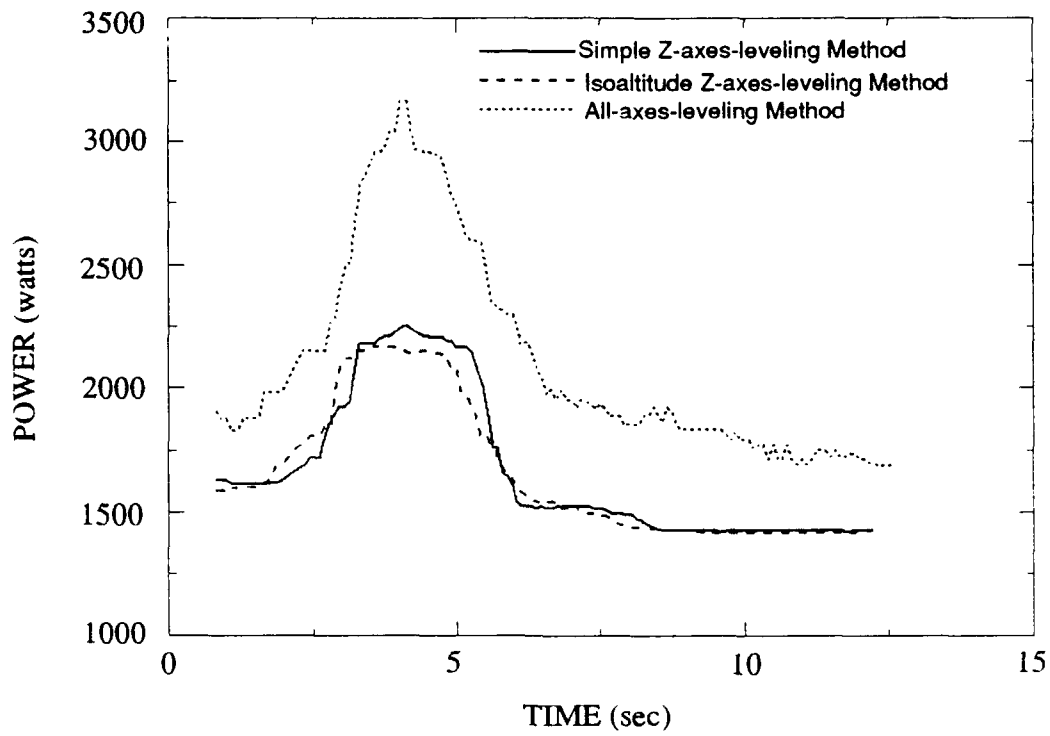


FIGURE 29. Power consumption for leveling the AMBLER from  $\theta = 3^\circ$  and  $\gamma = 3^\circ$

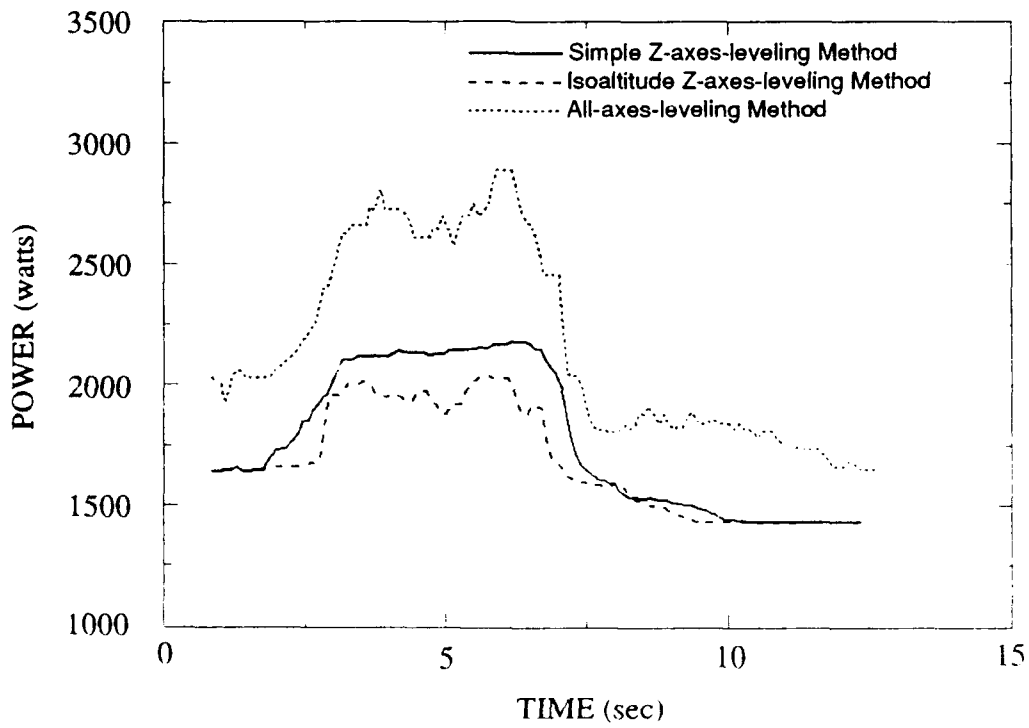


FIGURE 30. Power consumption for leveling the AMBLER from  $\theta = 5^\circ$  and  $\gamma = 5^\circ$

**TABLE 7.** Power meter data during the experiments

	All-axes Method (kW)	Z-axes Methods (kW)
Amplifiers, Lights, Electronics, misc. Housekeeping Power	1.42	1.42
Releasing Brakes	0.58	0.19
Mechanical Power	1.05	0.65
Total Power	3.05	2.26

## 5. Conclusion

Four different leveling methods have been simulated and implemented on the AMBLER. All of them achieve leveling and require different amounts of power. The difference in power consumption is a function of the amount that the body is lifted. However, it is affected even more by the number of actuators used by the leveling algorithm. Therefore, the All-axes-leveling method requires the most energy.

The Z-axes leveling methods do not compensate for the change in horizontal link lengths that are required to maintain relative foot contact positions. Consequently, the body of the walker translates and foot slippage is predicted. This phenomena is obscured by flexure in the legs and body. Foot slippage was detected when footholds were at dissimilar elevations. For very rough terrain or steep slopes, where the machine has very different foot elevations, it might be necessary to use the All-axes-leveling method, which theoretically compensates for foot slippage. Use of the All-axes leveling method may also be required to avoid foot slippage with a more rigid machine.

All of the Z-axes-leveling methods are good enough for leveling the AMBLER while on relative flat terrain, but the Isoaltitude Z-axes-leveling method exhibits the best performance based on power consumption and body frame motion.

Further research could be done in order to improve the power consumed due to releasing the brakes and driving the friction in joints. This would then make the All-axes leveling method more attractive from the energy viewpoint. Other research that would impact power consumption is the development of a regenerating energy storage system.

## 6. References

- [1] J. Bares and W. Whittaker, "Configuration of an Autonomous Robot for Mars Exploration," *Proc. World Robotics Conference*, Society of Mechanical Engineers, Gaithersburg, Maryland, May 7-11, 1989, pp. 1:37-1:52.
- [2] J. Bares and W. Whittaker, "Walking Robot with a Circulating Gait," *Proc. IEEE International Workshop on Intelligent Robots and Systems*, Tsuchiura, Japan, July 1990, pp. 809-816.
- [3] D. M. Gorinevsky and A. Y. Shneider, "Force Control in Locomotion of Legged Vehicles over Rigid and Soft Surfaces," *The International Journal of Robotics Research*, Vol. 9, No. 2, April 1990, pp. 4-23.
- [4] Y. Ishino et. al., "Walking Robot for Underwater Construction," *Proc. '83 ICAR*, Tokyo, Japan, Sep. 12-13, 1983, pp. 107-114.
- [5] M. Kaneko, K. Tanie and M. Than, "A Control Algorithm for Hexapod Walking Machine Over Soft Ground," *IEEE Journal of Robotics and Automation*, Vol. 4, No. 3, June 1988, pp. 294-302.
- [6] C. A. Klein, K. W. Olson and D. R. Pugh, "Use of Force and Attitude Sensors for Locomotion of a Legged Vehicle over Irregular Terrain," *The International Journal of Robotics Research*, Vol. 2, No. 2 Summer, 1982, pp. 3-17.
- [7] E. Krotkov, C. Caillas, M. Hebert, I.S. Kweon and T. Kanade, "First results in Terrain Mapping for a Planetary Explorer," *Proc. NASA Conference on Space Telerobotics*, Jet Propulsion Lab, Pasadena, CA, January, 1989.
- [8] E. Krotkov, R. Simmons and C. Thorpe, "Single-Leg Walking with Integrated Perception, Planning and Control," *Proc. IEEE International Workshop on Intelligent Robots and Systems*, Tsuchiura, Japan, July, 1990.
- [9] P. V. Nagy, "Motion Control for Multi-legged Walking Vehicles on Rugged Terrain," Ph.D. Thesis Proposal, Dept. of Mechanical Engineering, Carnegie Mellon University, Pittsburgh, PA, June 7, 1990.
- [10] P. Nagy, B. X. Wu and K. Dowling, "A Testbed for Attitude Control of Walking Robots." ISMM International Symposium on Computer Applications in Design, Simulation and Analysis, Las Vegas, NV, March 19-21, 1991, pp. 120, 123
- [11] R. Simmons, J. L. Lin and C. Fedor, "Autonomous Task Control for Mobile Robots." *Proc IEEE Symposium on Intelligent Control*, Philadelphia, PA, September, 1990.
- [12] R. Simmons and E. Krotkov, "An Integrated Walking System for the AMBLER Planetary Rover," *Proceedings of the 1991 IEEE International Conference on Robotics and Automation*, Sacramento, California, April 9-11, 1991, pp. 2086-2091.